The Hip

Anatomy, pathology and hip replacements

Anatomy

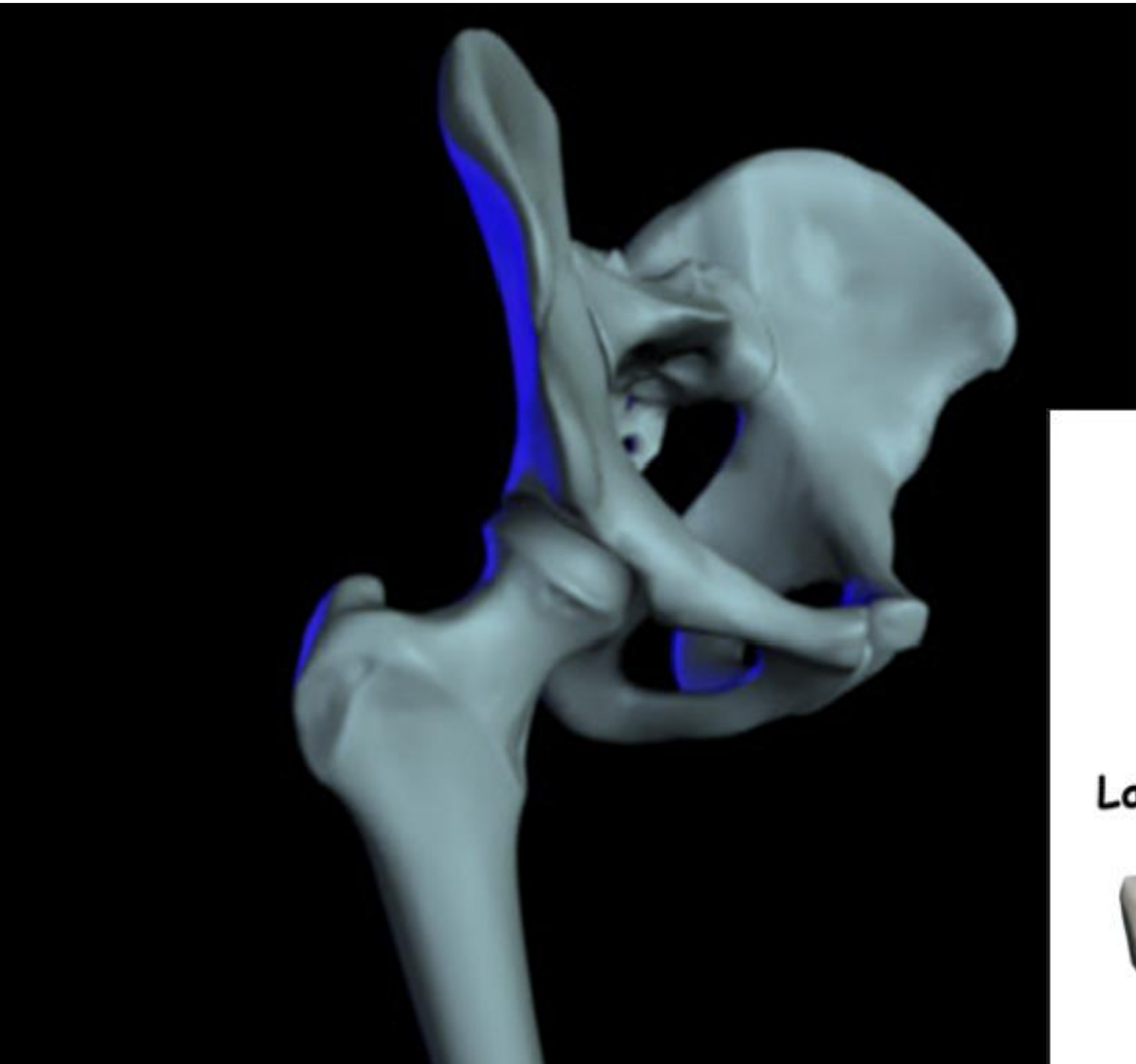

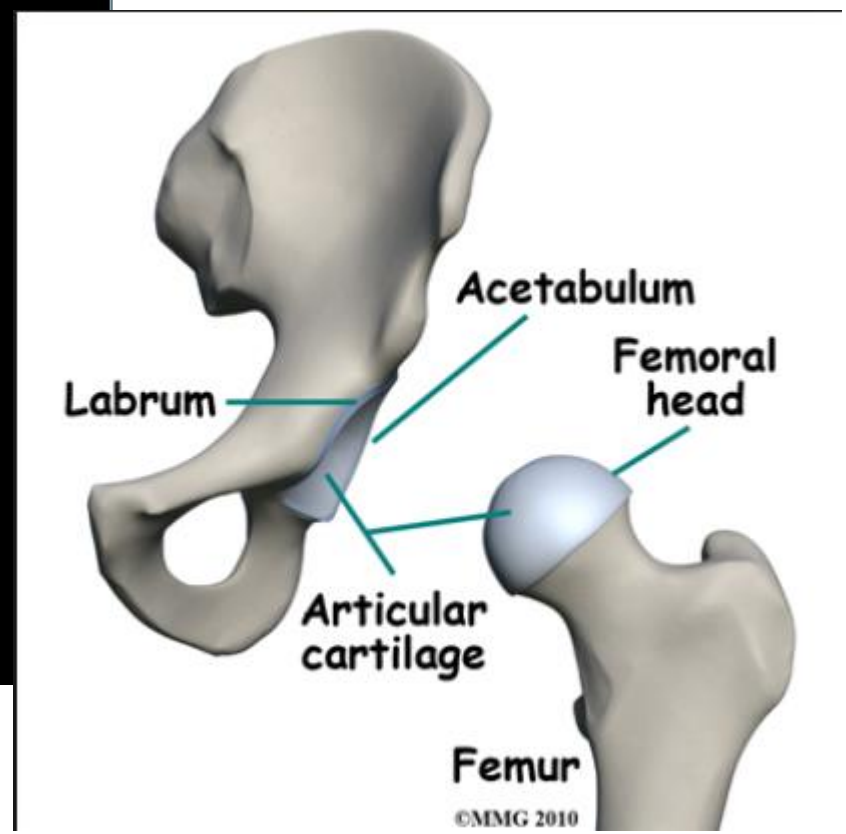
Acetabulum
Femoral head
Labrum
Articular cartilage
Femur
©MMG 2010

Ligaments of the Hip

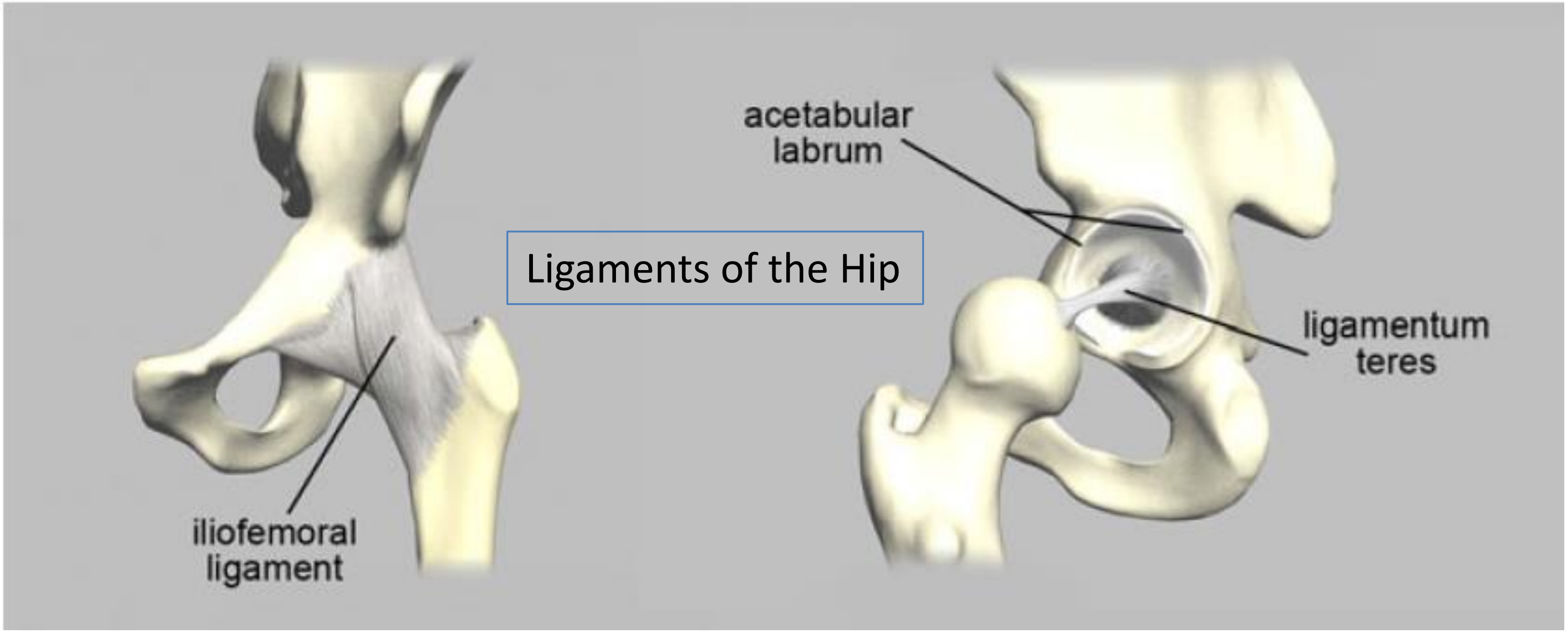

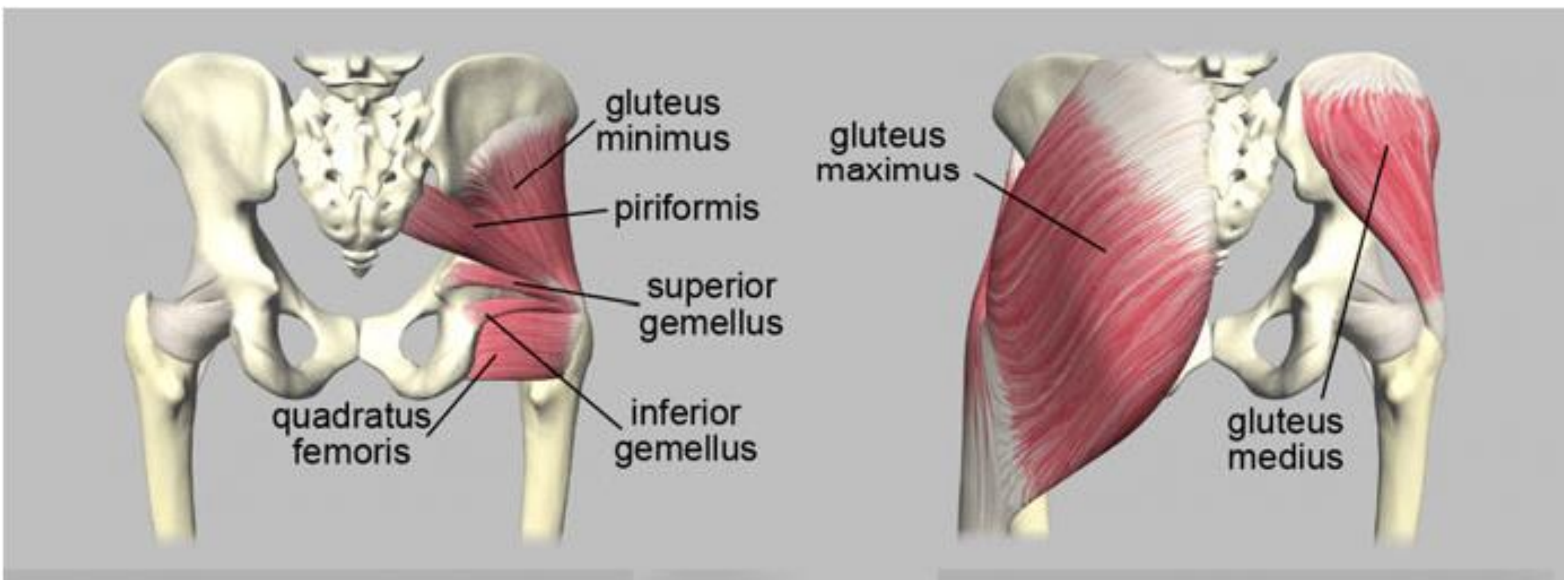

Anterior Hip Musculature

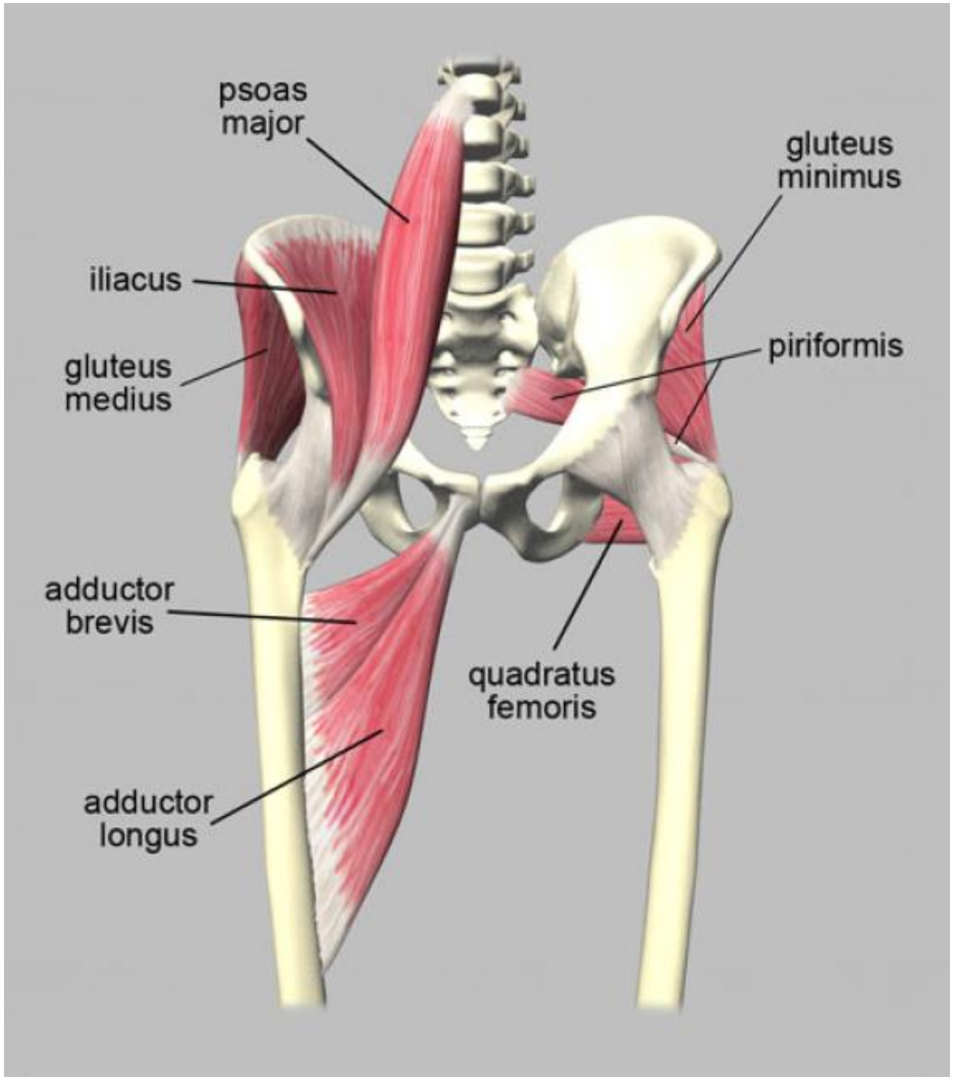

Biomechanics

Kinematics

Rotational Motions of the Hip

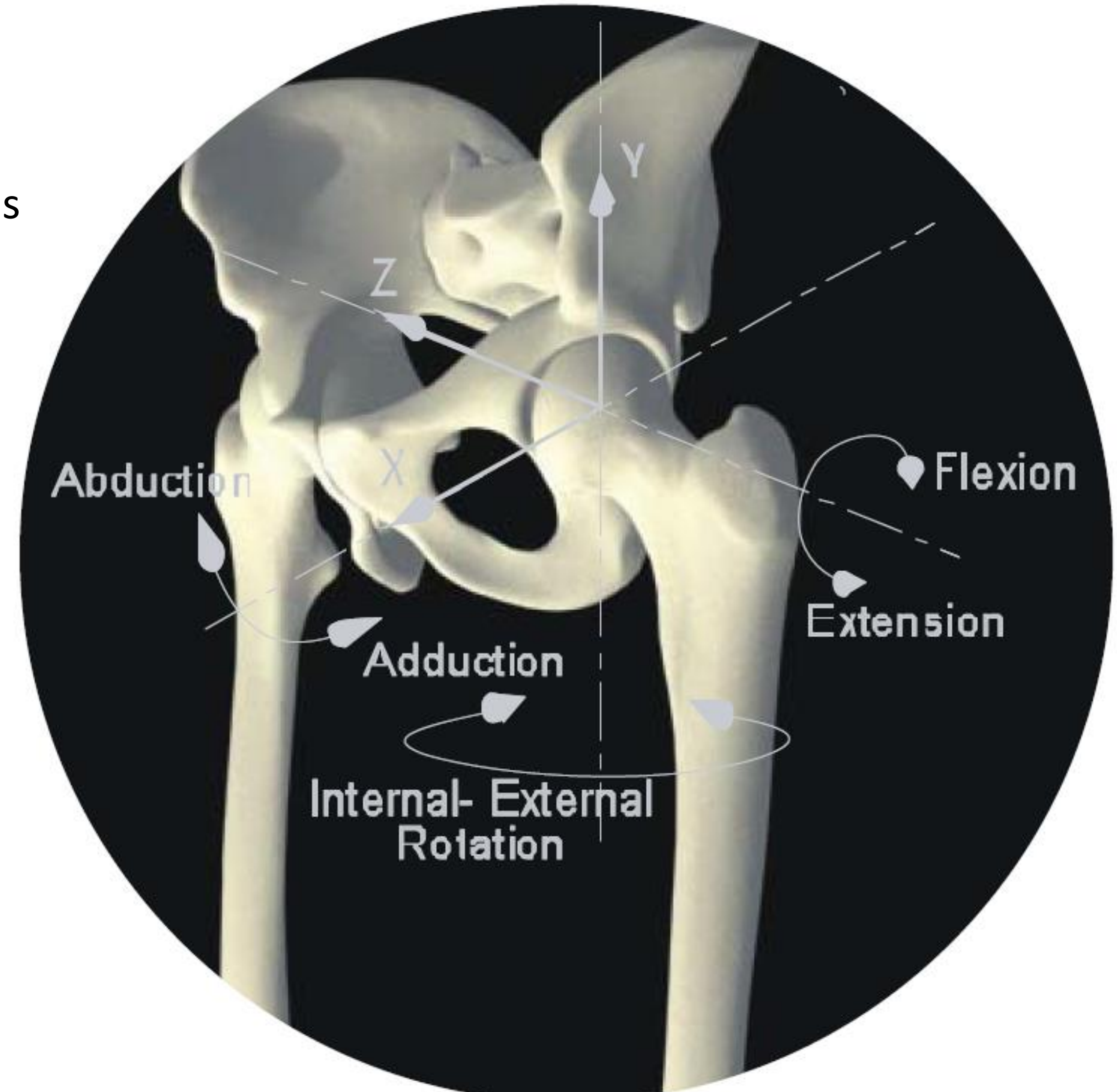

Range of motion

Normal mean range of motion (ROM) varies slightly, by about 3-5° with gender and race. Individual variations within groups are somewhat greater. The normal mean ROM in individuals in the 60 – 74 year age group (the most likely to have a hip replacement) is 118°(13° SD) flexion, 17°(8° SD) extension, 39°(12° SD) abduction, 30°(7° SD) internal rotation and 29°(9° SD) external rotation

Stability

The hip is a stable ball and socket joint and, thus, is constrained against significant translation motion and unconstrained against rotary motion except as limited by adjacent tissue.

Forces

Maximum compressive forces in the hip in relatively young normal males have been estimated to be on the order of five times body weight during normal walking.

During level walking it is estimated that the vertical component of the force on the femoral head is about 5BW, the A\P component about 2BW acting anteriorly and the M\L component about ≈BW medially

Degenerative diseases – Hip joint

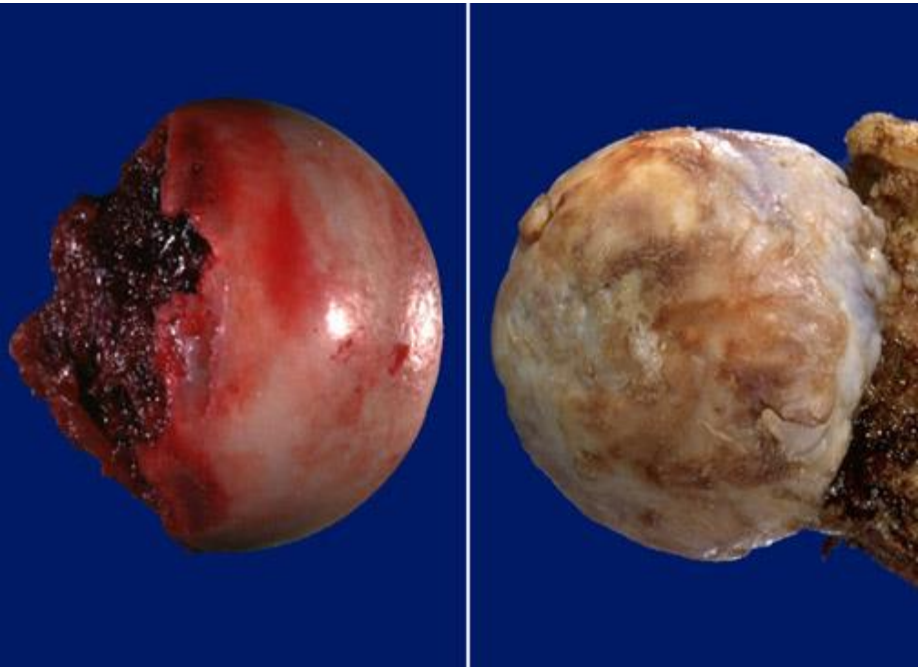

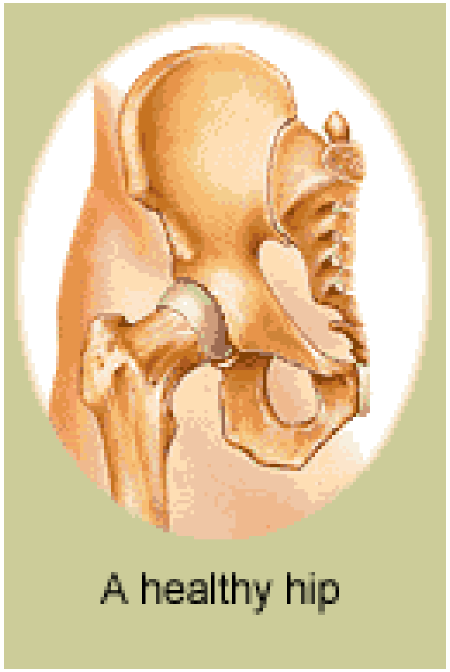

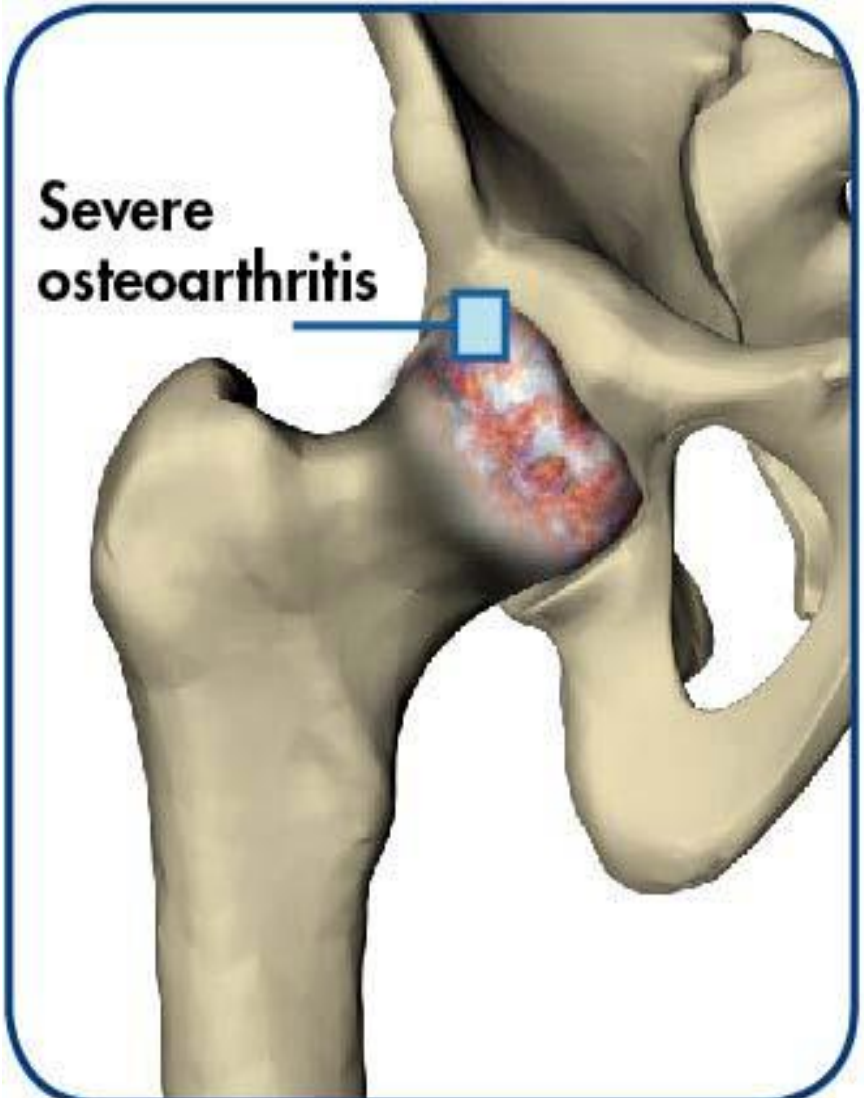
Severe
osteoarthritis

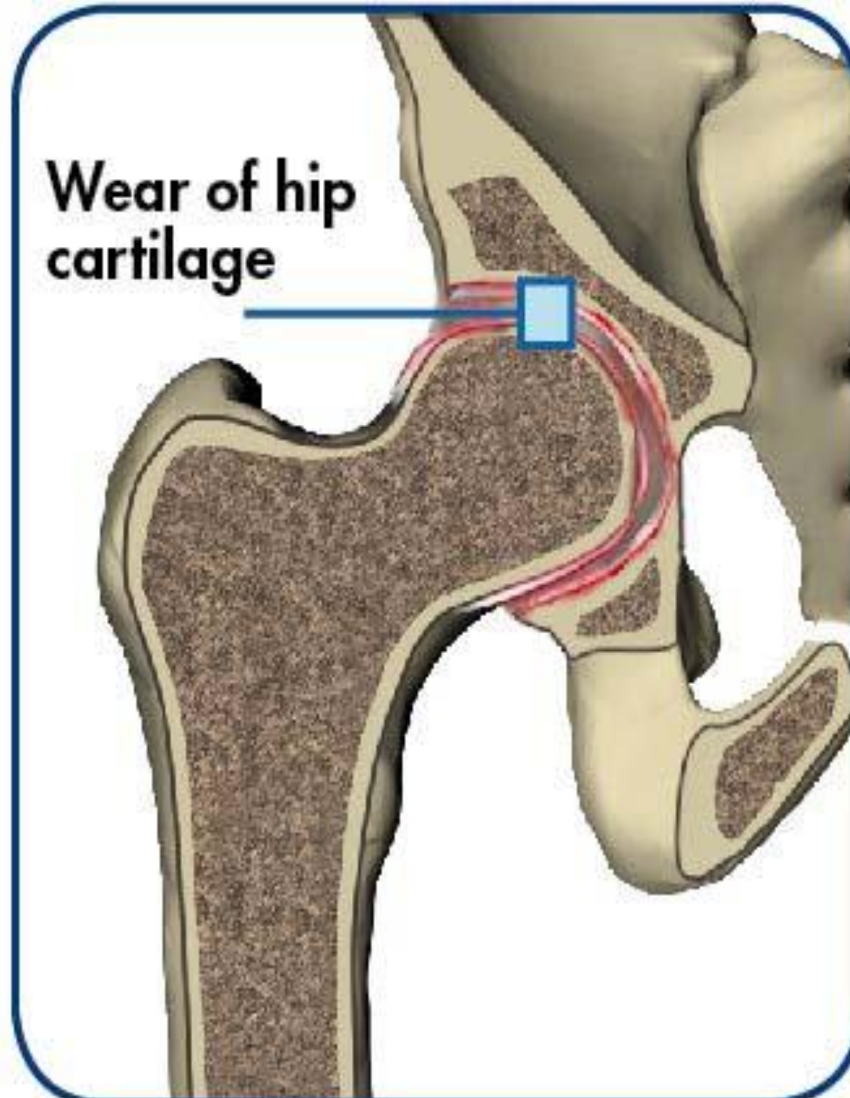
Wear of hip
cartilage

The steps involved in replacing a diseased hip with an uncemented artificial hip begin with making an incision on the side of the thigh to allow access to the hip joint.

Reference: Medical Multimedia Group (http://www.sechrest.com/mmg/)

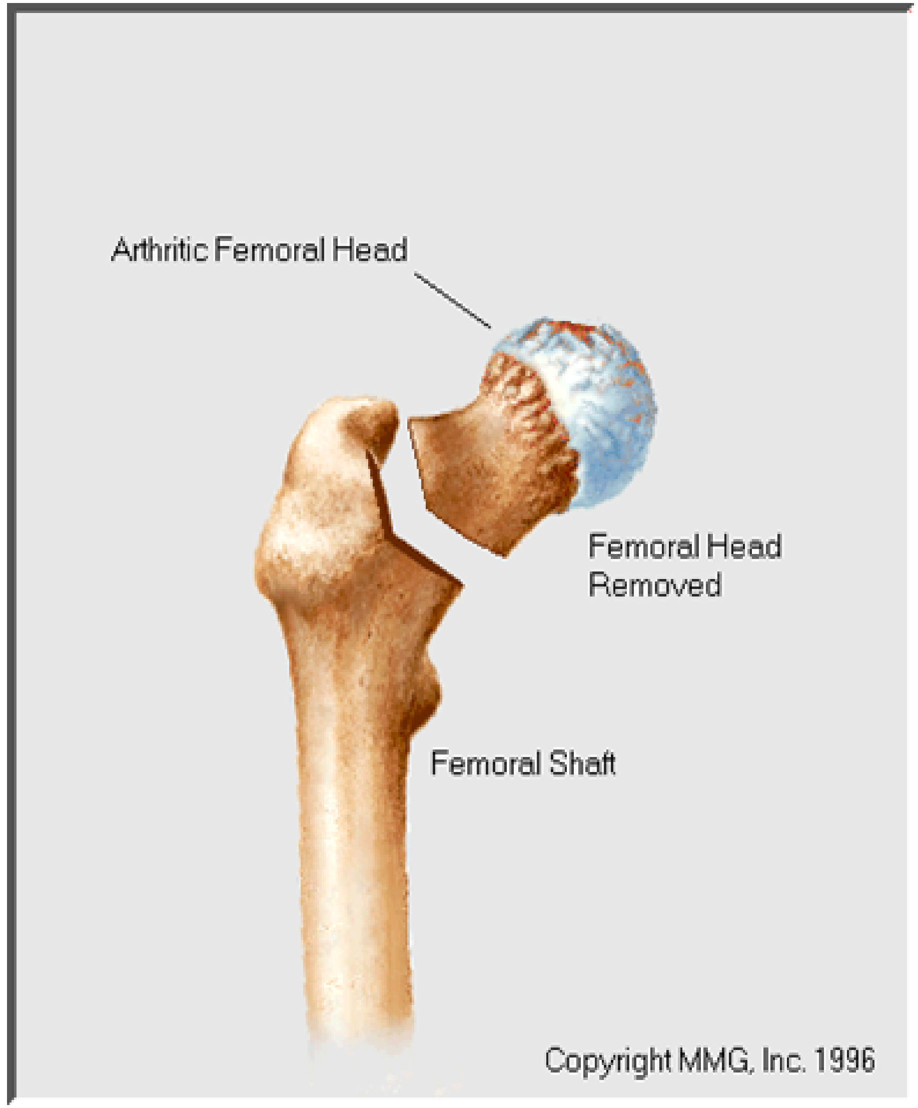

Removing the Femoral Head

Once the hip joint is entered, the femoral head is actually dislocated from the acetabulum and the femoral head is removed by cutting through the femoral neck with a power saw.

Reaming the Acetabulum

Attention is then turned towards the socket, where using a power drill and a special reamer, the cartilage is removed from the acetabulum and the bone is formed in a hemisperical shape to exactly fit the metal shell of the acetabular component.

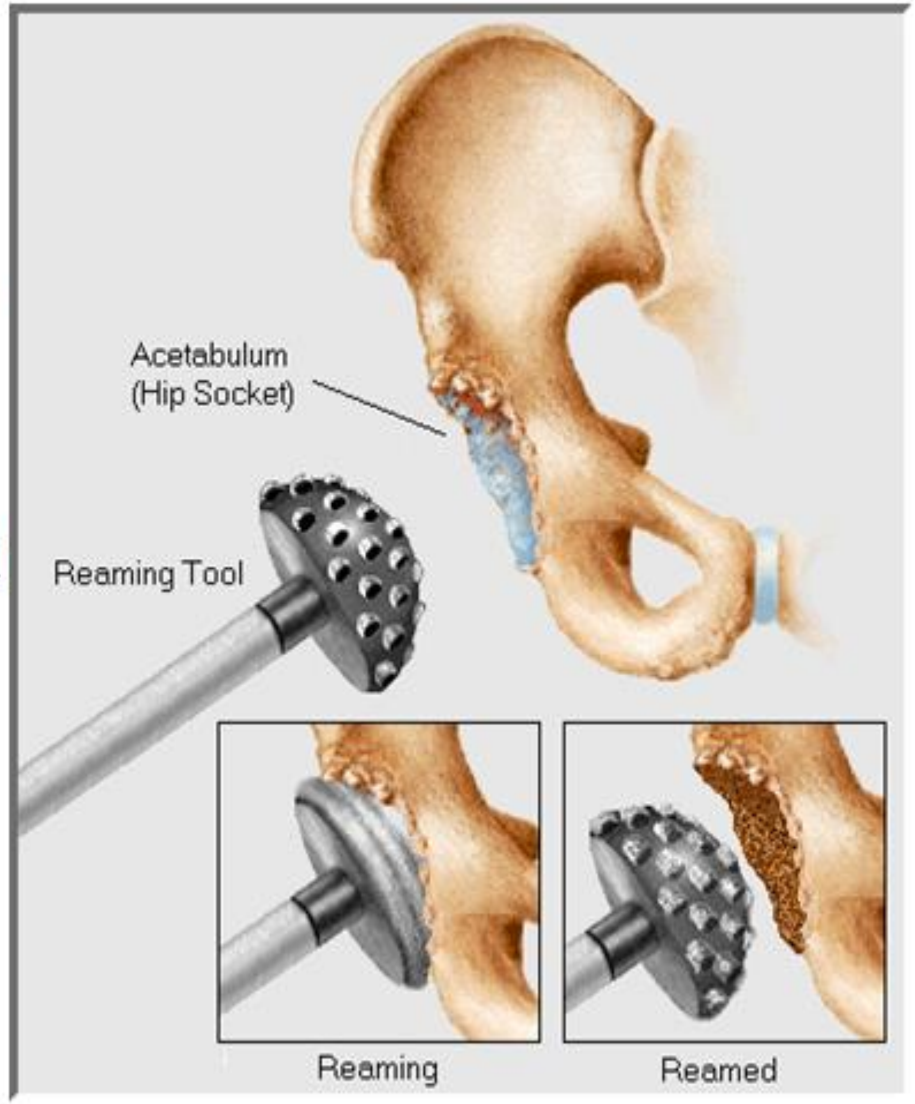

Inserting the Acetabular Component

Once the right size and shape is determined for the acetabulum, the acetabular component is inserted into place. In the *uncemented* variety of artificial hip replacement, the metal shell is simply held in place by the tightness of the fit or by using screws to hold the metal shell in place. In the *cemented* variety, a special epoxy type cement is used to anchor the acetabular component to the bone.

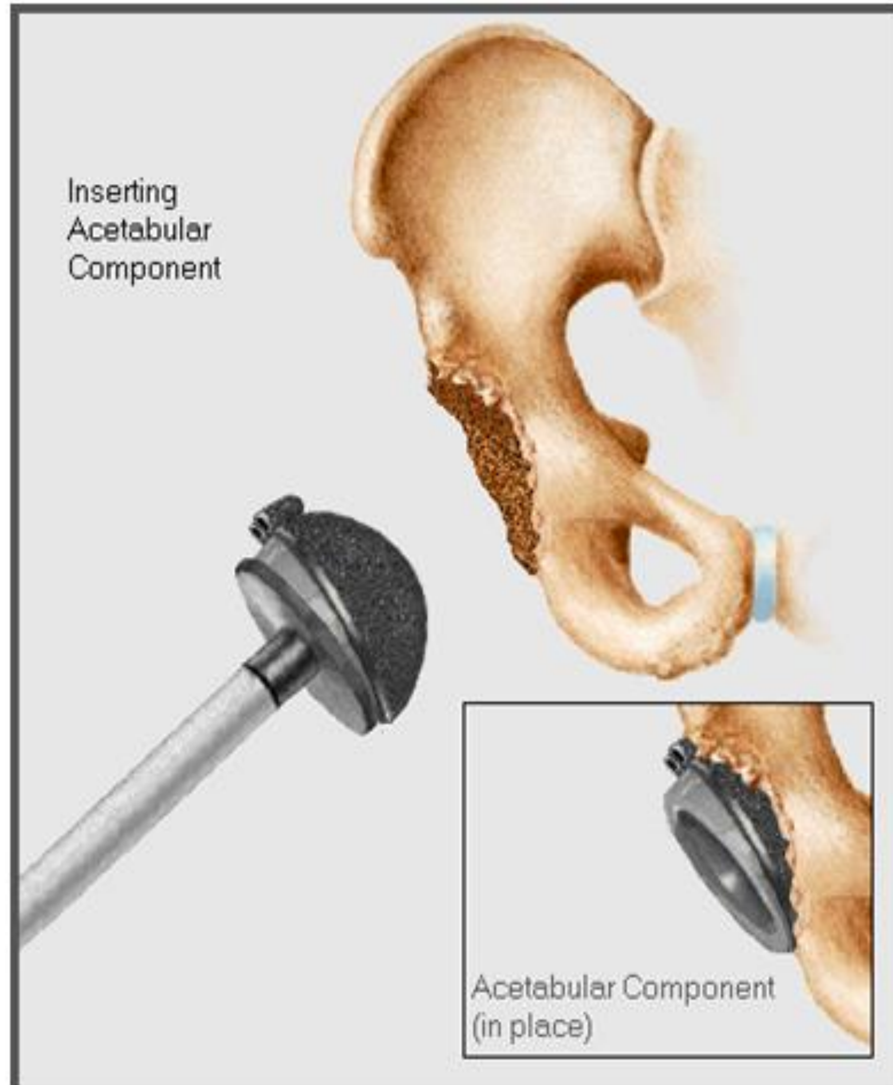

Preparing the Femoral Canal

To begin replacing the femur, special rasps are used to shape the hollow femur to the exact shape of the metal stem of the femoral component.

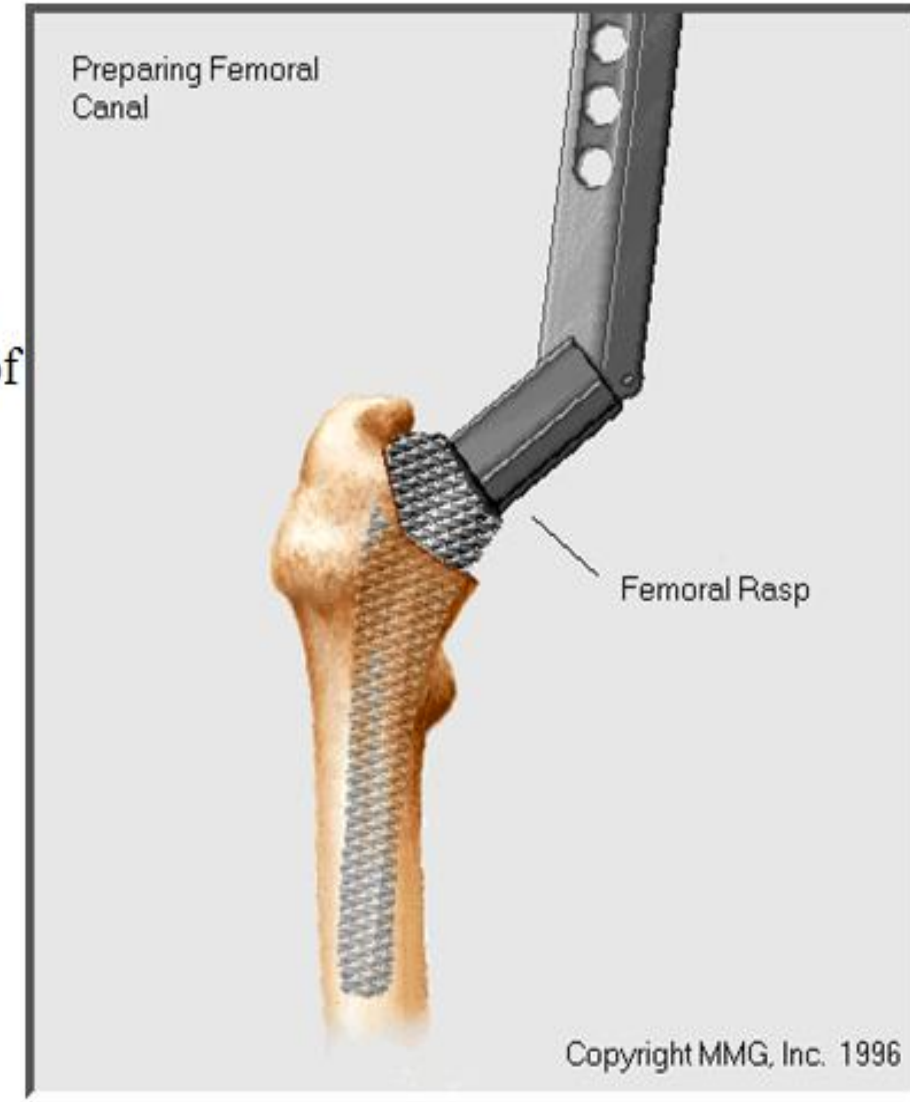

Inserting the Femoral Stem

Once the size and shape are satisfactory, the stem is inserted into the femoral canal. Again, in the *uncemented* variety of femoral component the stem is held in place by the tightness of the fit into the bone (similar to the friction that holds a nail driven into a hole drilled into wooden board - with a slightly smaller diameter than the nail). In the *cemented variety*, the femoral canal is rasped to a size slightly larger than the femoral stem, and the epoxy type cement is used to bond the metal stem to the bone.

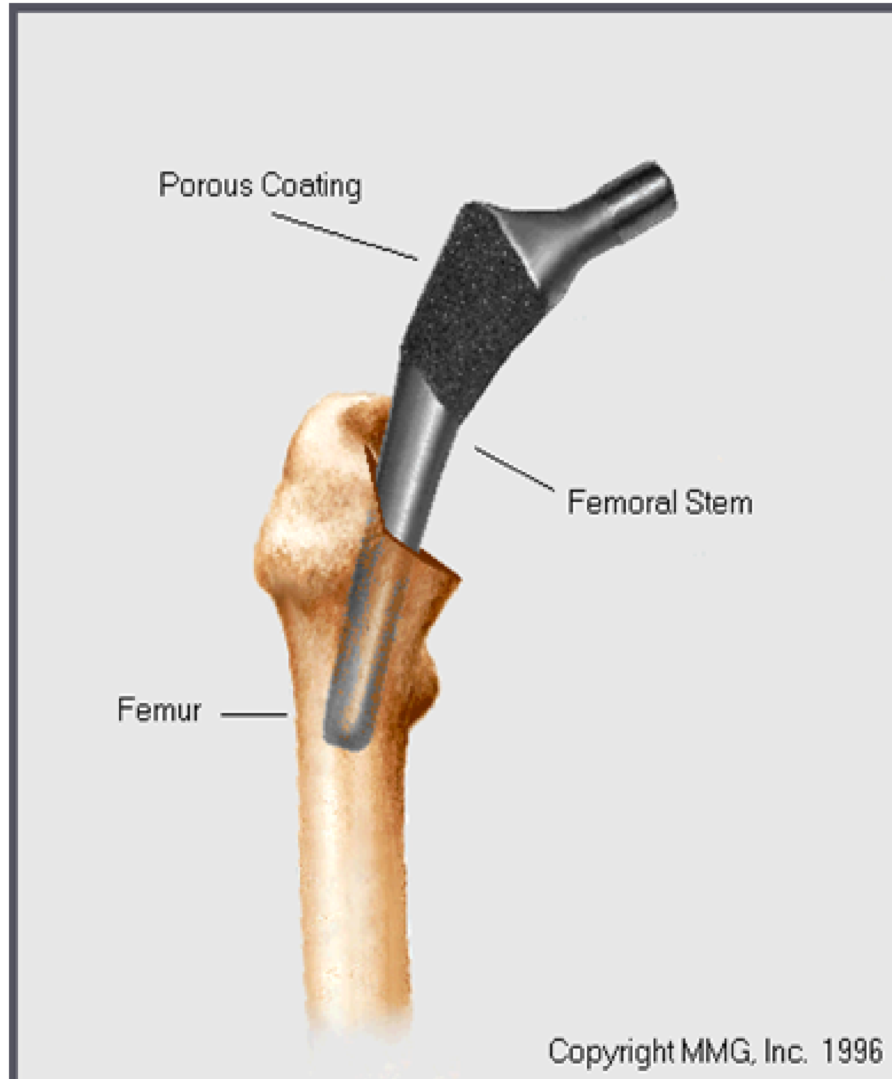

Attaching the Femoral Head

The metal ball that makes up tl
femoral head is attached.

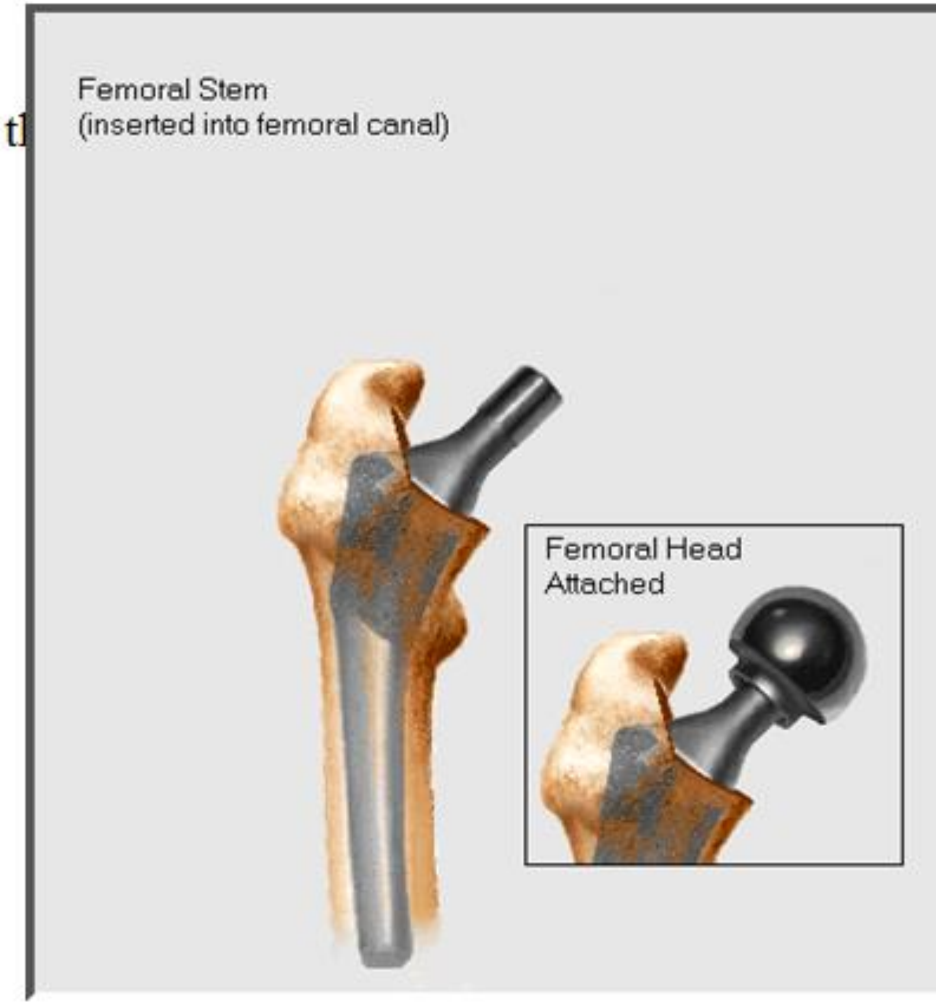

The Completed Hip Replacement

And, voila!, you have a new bearing surface for the diseased hip.

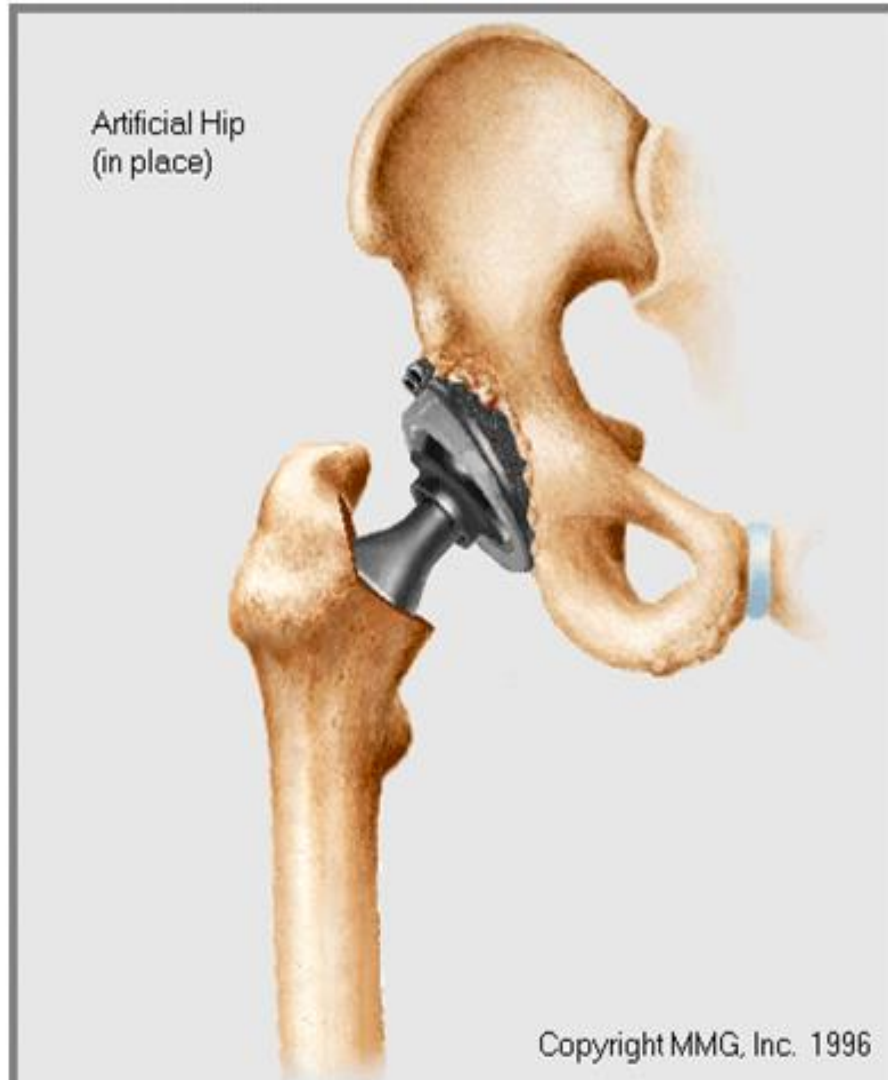

Total Hip Replacement

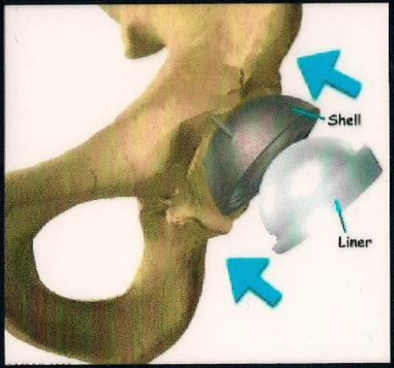

Artificial joints

A. Fixation with cement
B. Cementless fixation

A

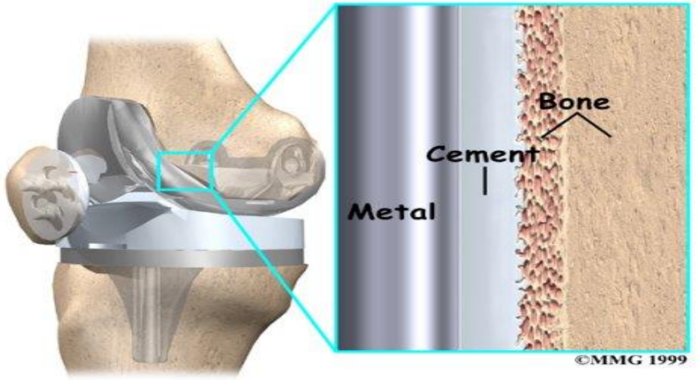

B

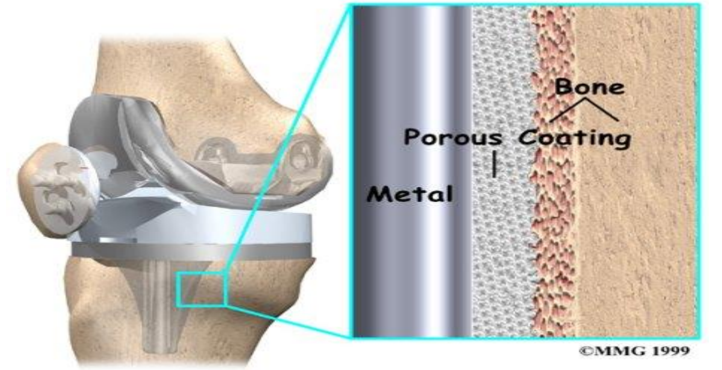

Problems

- chemical, thermical, mechanical trauma due to in situ PMMA polymerization
- repetition of surgery
- mechanical instability at polymer-bone or polymer-metal with time

Possible solution

Materials of types II, III

Stresses from completely bonded to unbonded

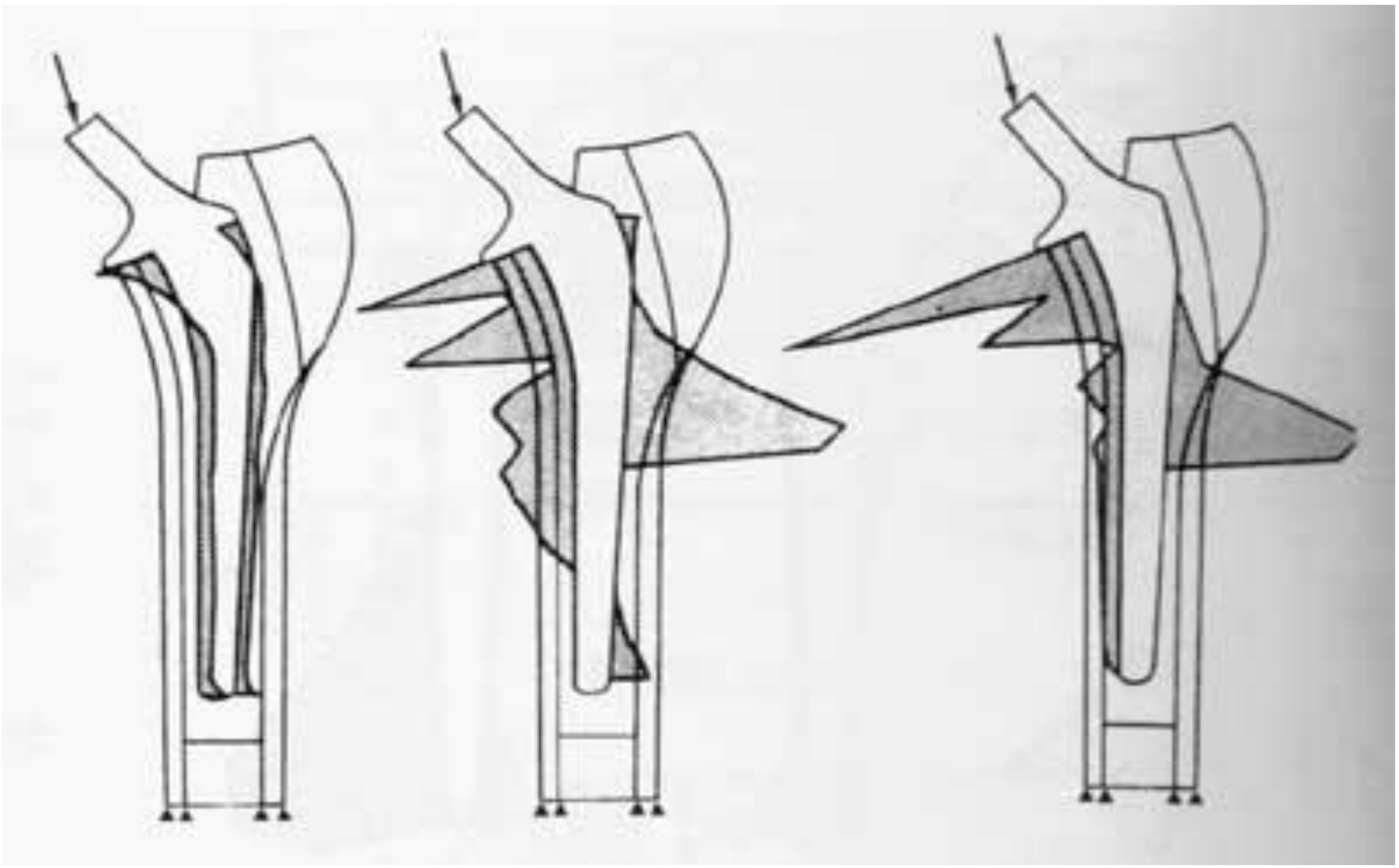

Artificial hip joint

Heads

Hip implant

Artificial hip joint

Stems

A

B

Stems designs

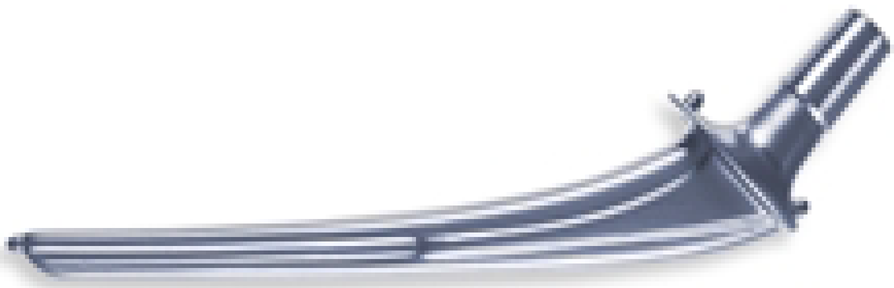

Lubinus SP II stems made of CoCr

Spectron EF, *Smith & Nephew*

Anatomic-Option, *Zimmer*

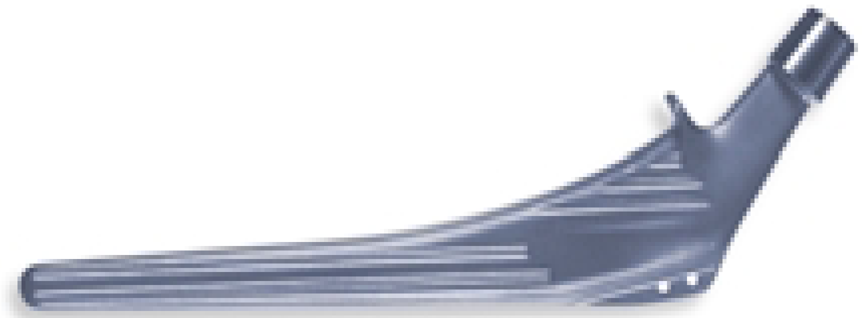

Tifit, *Smith & Nephew*

Exeter, *Stryker-Howmedica*

Artificial hip joint

Cups

A

B

19. Material combination in current use for joint prostheses

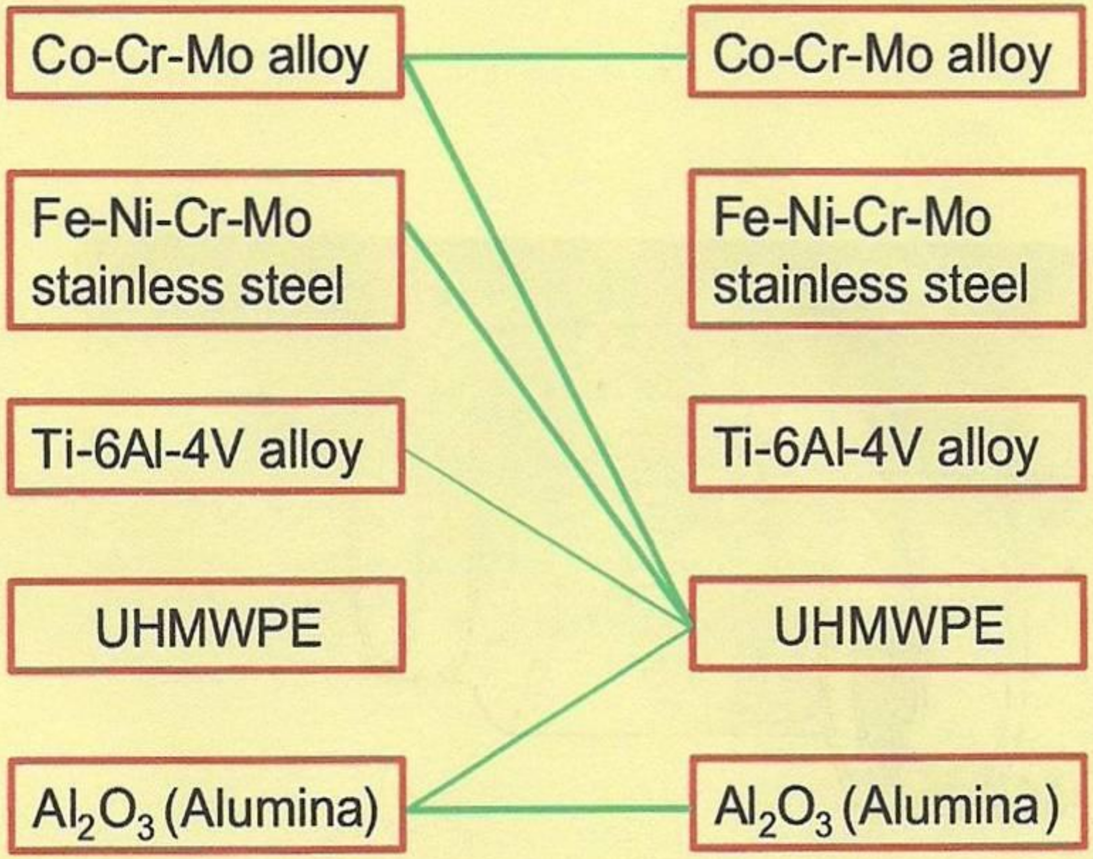

20. Material combination in artificial hipjoint

Material of head	Materials of cup						
	Polymers					Metal	Ceramics
	PTFE	UNMWPE	TFCE	POM	PETF	CoCrMo	Al_2O_3
FeCrNiMo	×	++	×	•	•	–	–
FeCrNiMoNbN	•	++	–	•	•	–	–
CoCrMo	•	++	×	×	×	++	–
TiAlV	•	×	×	–	–	–	–
Al_2O_3	•	++	•	•	•	–	++
ZrO_2	•	+	•	•	•	–	–

++ clinicaly tested for many years

+ undergoin clinical tested

-technical unfit

x clinical unfit

* not study

Material selection

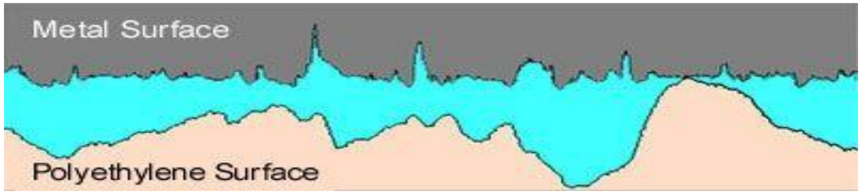

Thick film lubrication is never possible in a metal-polyethylene or ceramic-polyethylene bearing because of the high surface roughness of polyethylene.

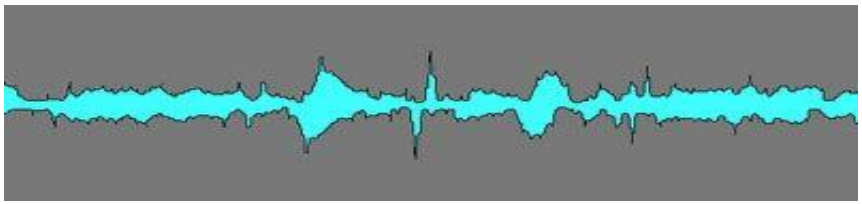

Thick film lubrication in M/M bearing. Synovial fluid completely separates articulating surfaces resulting in low friction & low wear

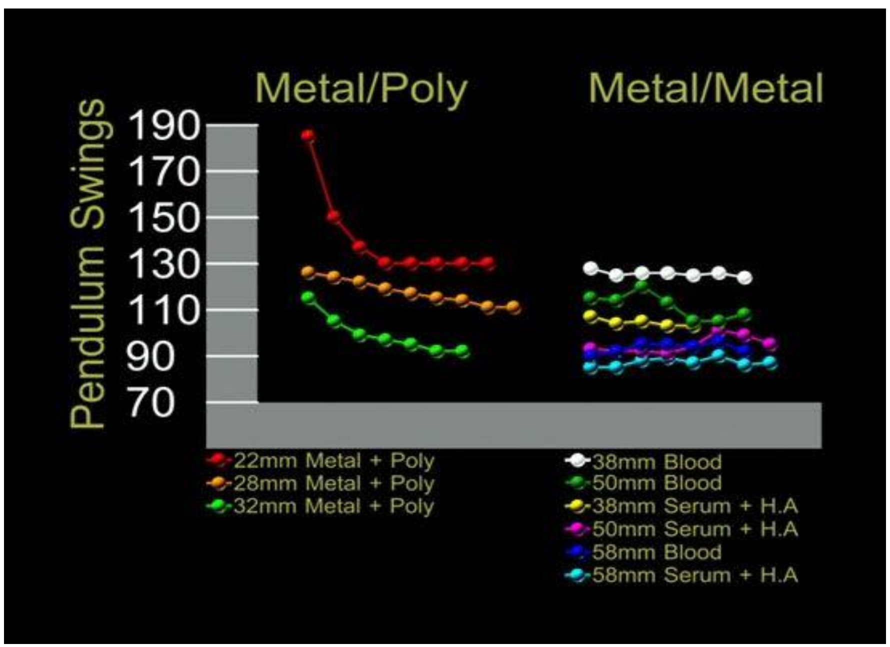

Bearing combination	Wear Rate
Metal-on-polyethylene	0.2 mm/year
Alumina-on-polyethylene	0.1 mm/year
Metal-on-metal	0.006 mm/year
Alumina-on-alumina	<0.001 mm/year

Titanium-Based Biomaterials for Preventing Stress Shielding between Implant Devices and Bone

Alloy	Young's modulus (GPa)	Tensile strength (MPa)
Co-Cr-Mo	230	1793
Ti-6Al-4V	110	860
Ti-35Nb-5Ta-7Zr	55	1030
Ti-29Nb-13Ta-4.6Zr	65	
Ti-Nb-Sn	‹ 55 (45.6)	>800
Human cortical bone	10-30	

Stress shielding

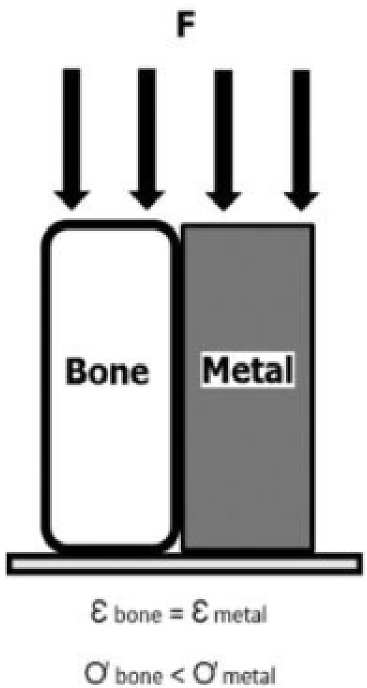

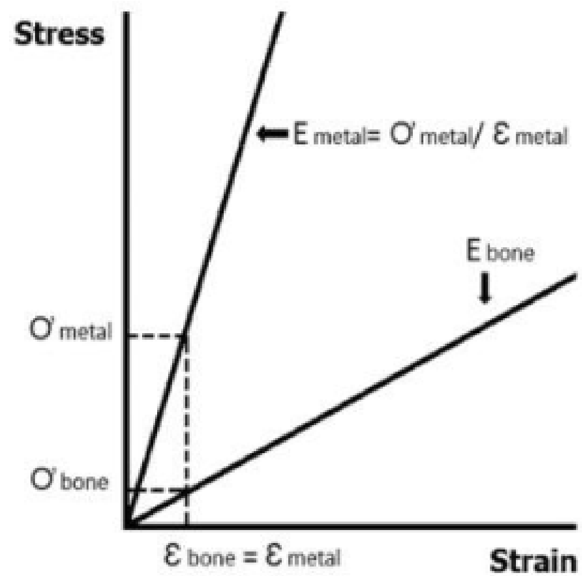

Mechanical biocompatibility - Stress shielding

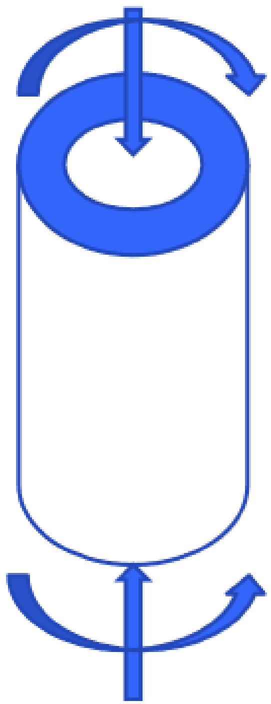

F=3000 N, 4 WB
M=30 Nm
D_i =1.1-1.5 cm, D_o=2.5 cm

Bone:	E=17 GPa
SS:	E=193 GPa
Co-Cr:	E=214 GPa
Ti-alloy:	E=124 GPa

Axial:
$$\sigma_b = \frac{E_b \cdot F}{E_b \cdot A_b + E_s \cdot A_s}$$

Bending:
$$\sigma_b = \frac{E_b \cdot M \cdot d_b / 2}{E_b \cdot I_b + E_S \cdot I_S}$$

Axial loading

Material	Core diameter, cm	Bone stress, MPa	Stem stress, MPa
Bone without implant		7.3	-
SS stem	1.1	2.0	23.1
SS stem	1.5	1.3	14.7
Co-Cr stem	1.5	1.2	14.9
Ti-alloy	1.1	1.9	13.6
Ti-alloy	1.5	2.8	20.1

Bending loading

Material	Core diameter, cm	Bone stress, MPa	Stem stress, MPa
Bone without implant		20.0	-
SS stem	1.1	14.0	70.4
SS stem	1.5	8.4	56.8
Co-Cr stem	1.5	7.8	69.0
Ti-alloy	1.1	10.8	47.0
Ti-alloy	1.5	15.8	50.8

Design Evolution

Early Arthroplasty

- Arthroplasty was first performed by several surgeons during the 19th century using human and animal tissue.
- The limited use of metal interposition was introduced and used in the late 19th and early 20th centuries with limited success. Smith-Peterson introduced the use of a glass interposition cup in 1923 - the door was cracked open to successful prosthetic arthroplasty of the hip.
- Total hip replacement was attempted by Gluck late in the 19th century using ivory components. In about 1958, Wiles used a metal ball and socket device.
- The unavailability of appropriate materials and a lack of understanding of mechanical design and biomechanics combined with a lack of understanding of the fixation prevented the development of successful total joint replacement in these early attempts.

First Generation Designs – Interposition Cups

a) The Smith-Peterson Cup

Refinement of the design by use of several different materials. He finally chose a Co-Cr-Mo alloy, which they called “Vitallium”.

a) Acetabular Interposition Cups

The McBride cup, in the late 1950’s, introduced interposition cups for essentially resurfacing the acetabulum

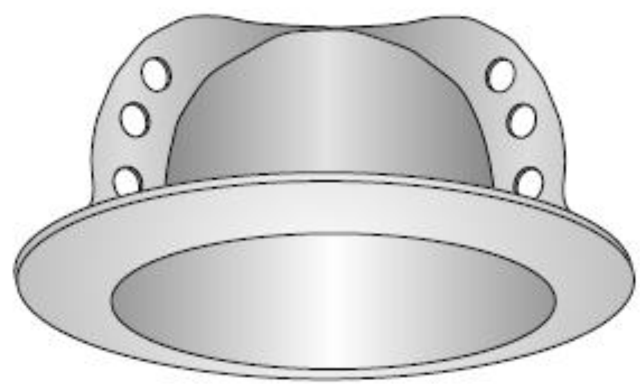

Second Generation Designs – Hemi Replacements

a. The Judet Surface Replacement
1946, acrylic head, later Co-Cr-Mo

b. Austin-Moore
Concepts of fixing a head replacement with an intramedullary straight stem by press fit into the femoral shaft.

c. The Thomson Femoral Component
The Thomson femoral component used a shorter curved stem

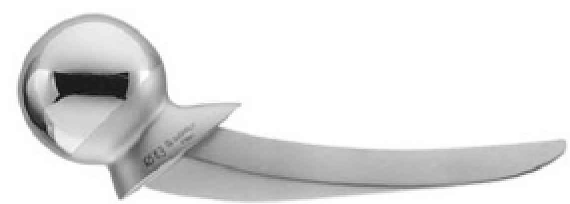

g) Surface Replacement

Several resurfacing total hip replacement designs were developed and used in the late 1960's and the 1970's. In general, they were unsuccessful and abandoned.

Hip resurfacing

Intervention

BHR compared with THR

The BHR

Third Generation Designs – Total Replacements

a) The McKee-Farrar Total Hip Replacement,
A variation of the Thompson femoral stem and an acetabular interposition cup

b) The Charnley Cemented Total Hip Replacement, 1969
Wear resistance, grouting agent for fixation of the prosthesis to bone

c) The Müller Total Hip Replacement, variations of the Charnley design

d) The Ring total Hip Replacement
Screw augmented press fit design

e) The Bipolar Acetabular Cup

f) Ceramic-on-Ceramic

Boutin introduced ceramic-on-ceramic articulation total hip replacement in the early 1970’s . These devices utilized both cemented and press fit acetabular components and a ceramic head on a femoral stem . Ceramic surfaces are hard, wear resistant and, most importantly, their wear products have much lower toxicity than UHMWPe or metal wear particles.

Problems:

acetabular loosening ,
ceramic fracture, and
squeaking

Self-Aligning Acetabular Component

Pappas and Buechel [1982] introduced the concept of "Positive Eccentricity", which allowed more predictable positioning of the cup on the stem and improved function.

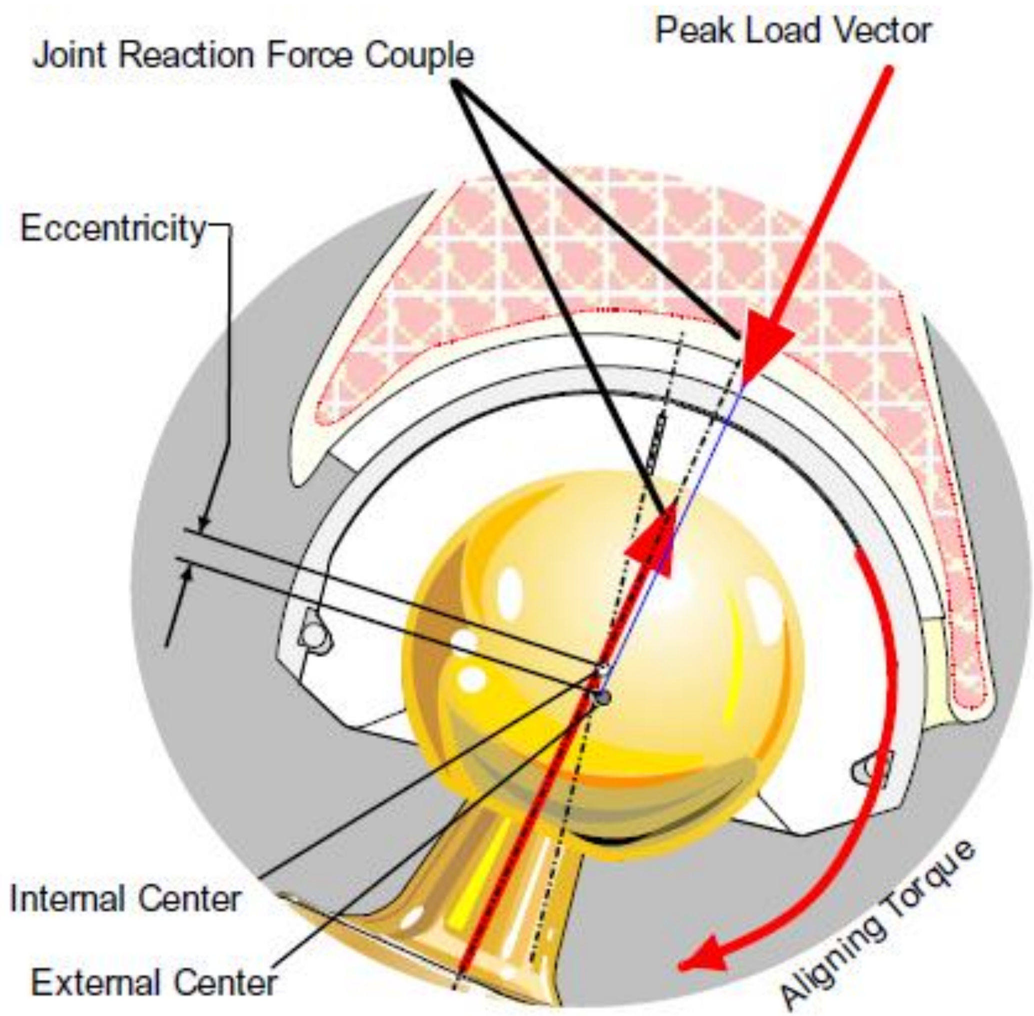

Fourth Generation Designs
Biological Fixation and Femoral Head Modularity

Fixation surfaces with relatively large mm size beads and fully coated stems. Later developments led to the use of small, sintered bead [1971] or plasma sprayed [1975] fibrous layered porous coating on femoral stems and acetabular cups.

a) Femoral Stems

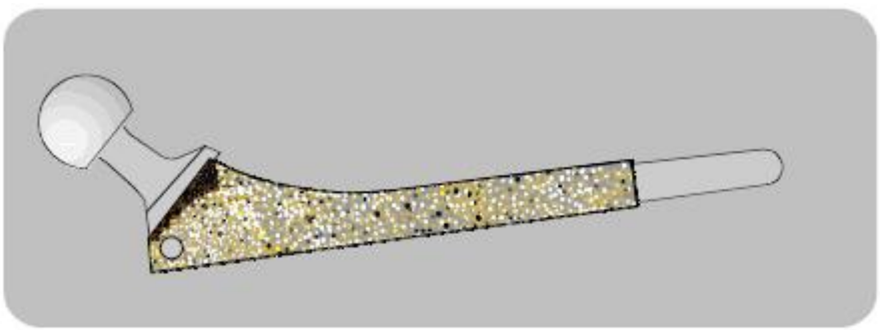

The AML Porous Coated Femoral Component using a straight stem for a decent press fit needed for biological fixation

b) Acetabular Cups

Use of a metal backed UHMWPe acetabular component augmented by screws

Fifth Generation Designs - Refinement

Improved material, manufacturing techniques and knowledge, provide opportunity for design refinement

The Buechel-Pappas Hip Replacement System [2004]: optimized femoral stem, proximal porous coating geometries to reduce stress shielding

Improvements

- Optimized femoral stem and proximal porous coating geometries $\rightarrow$ reduce stress shielding and minimize thigh pain.
- Thin-film ceramic surface coatings $\rightarrow$ significant improvements in wear resistance when used for articulation with UHMWPe .
- Entire porous coated prosthesis $\rightarrow$ reduces the surface exposure of the prosthesis avoiding increased metal ion release without preventing bone ingrowth.
- Thin-film ceramic coating on a relatively soft substrate like titanium (Ti-6Al-4V) alloy hardens the surface against scratching from bone or third
- body abrasive particles $\rightarrow$ extending the use of titanium alloys for orthopaedic implant.
- The development of highly cross-linked UHMWPe appears to substantially reduce wear in metal to plastic articulations.

EVALUATION

Prerequisites for successful total hip arthroplasty are long-term fixation and function, together with excellent wear resistance

Evaluation of the success or failure of one hip replacement system over another – retrieval analysis

- Survivorship analysis
- Radiographic analysis
- Clinical results

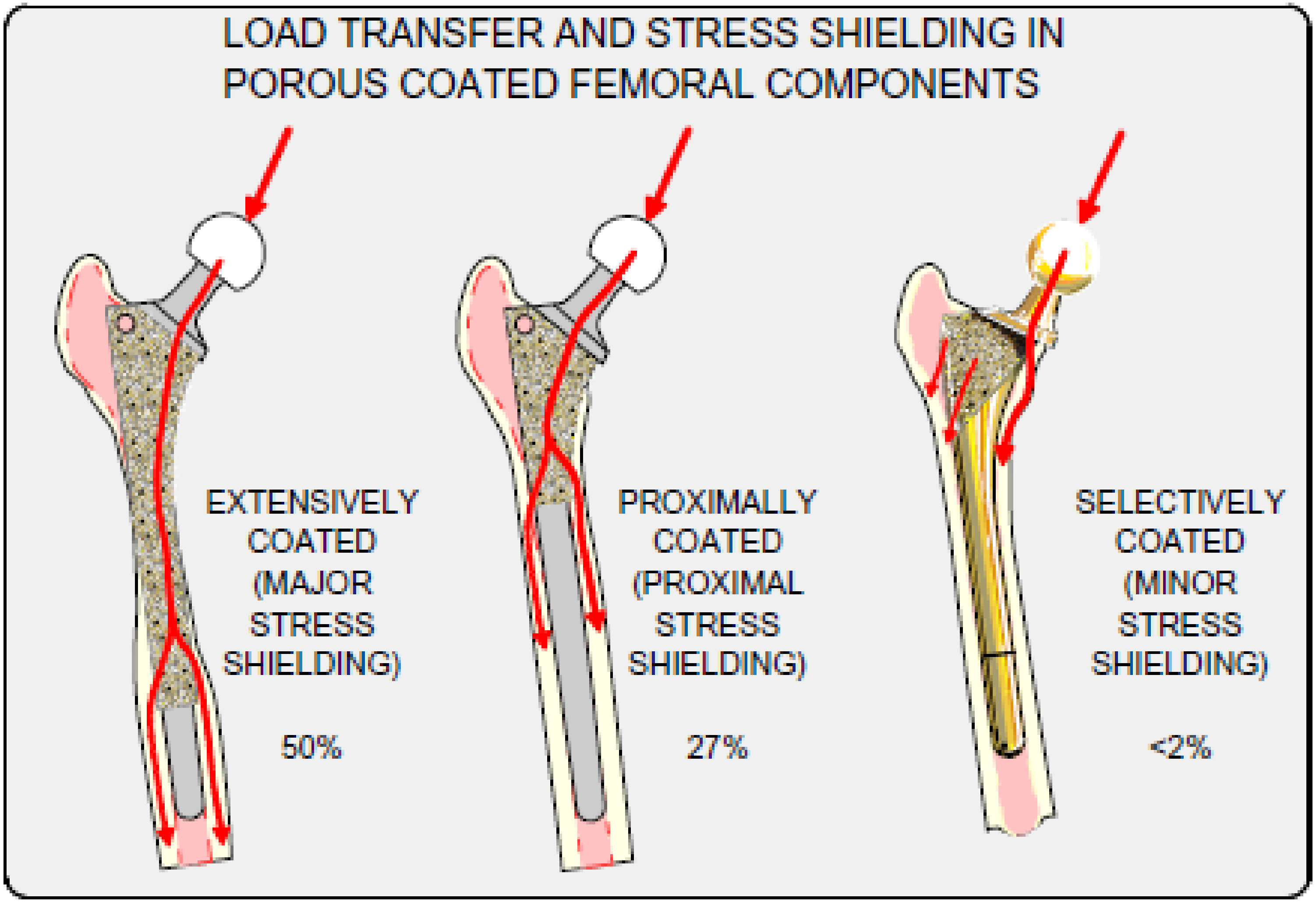

Effect of Degree of Porous Coating on Stress Shielding –
Ideal ingrowth for maintaining stability while minimizing stress shielding

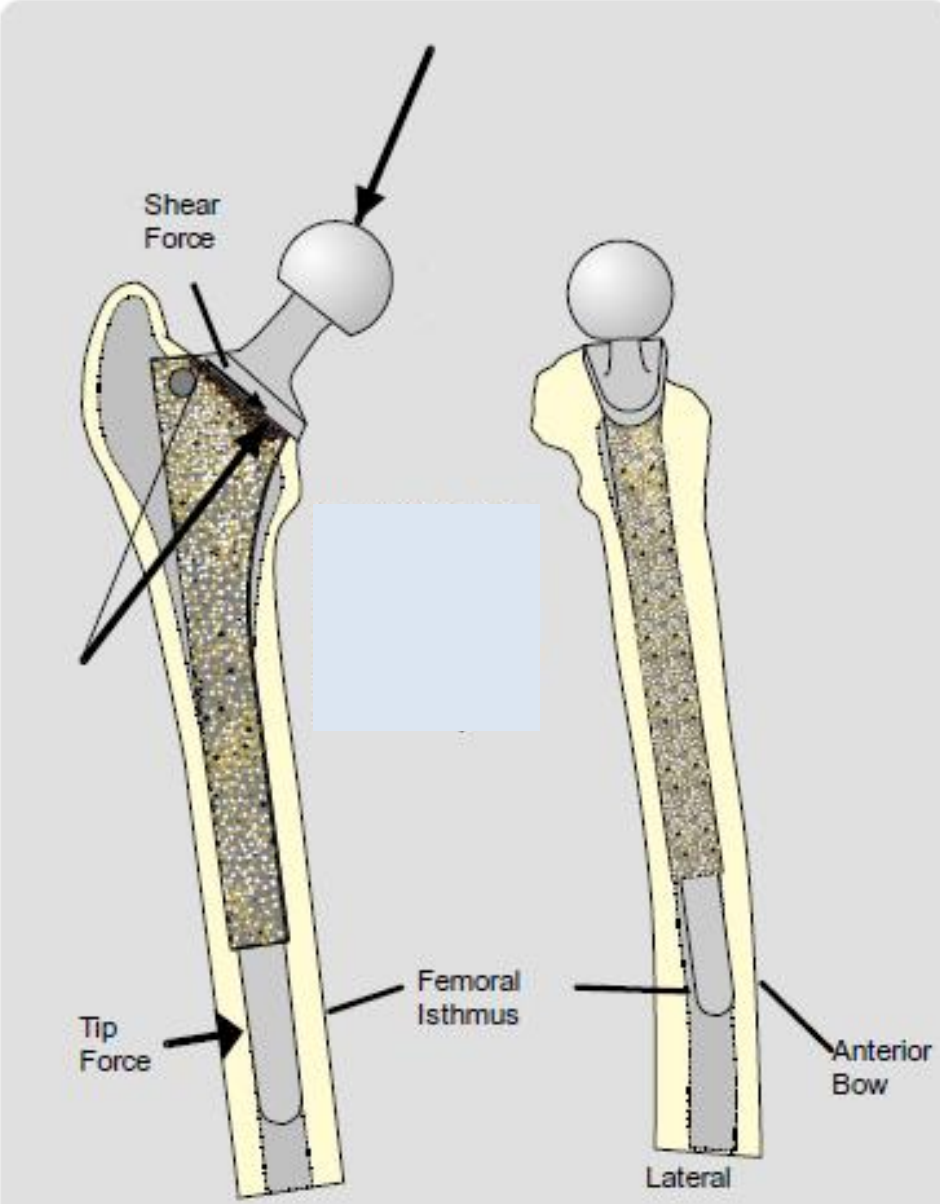

Causes Extensive Anterior Bow
and Isthmus Contact
Contributes to Thigh Pain

Long, stiff femoral stems that impinge at the femoral bow, and have non-optimal 45° loading collars contribute to thigh pain. As it is not perpendicular to peak load vector, a shear force is developed resisting by a stem tip force, increasing lateral endosteal load and causing thigh pain.

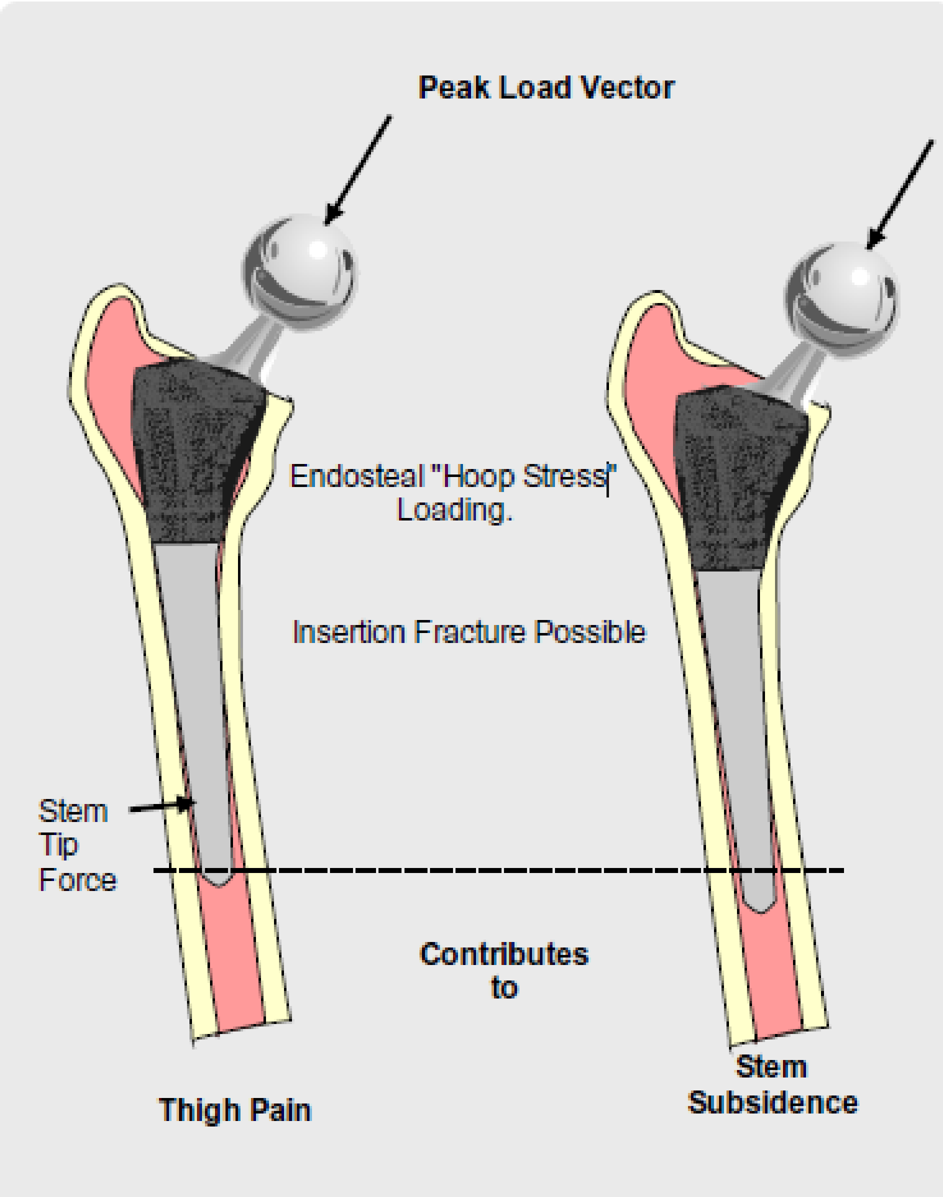

Collarless stem showing initial implant position, along with subsided position contributing to thigh pain or uncontrolled leg length shortening.

Design of the B-P Hip System

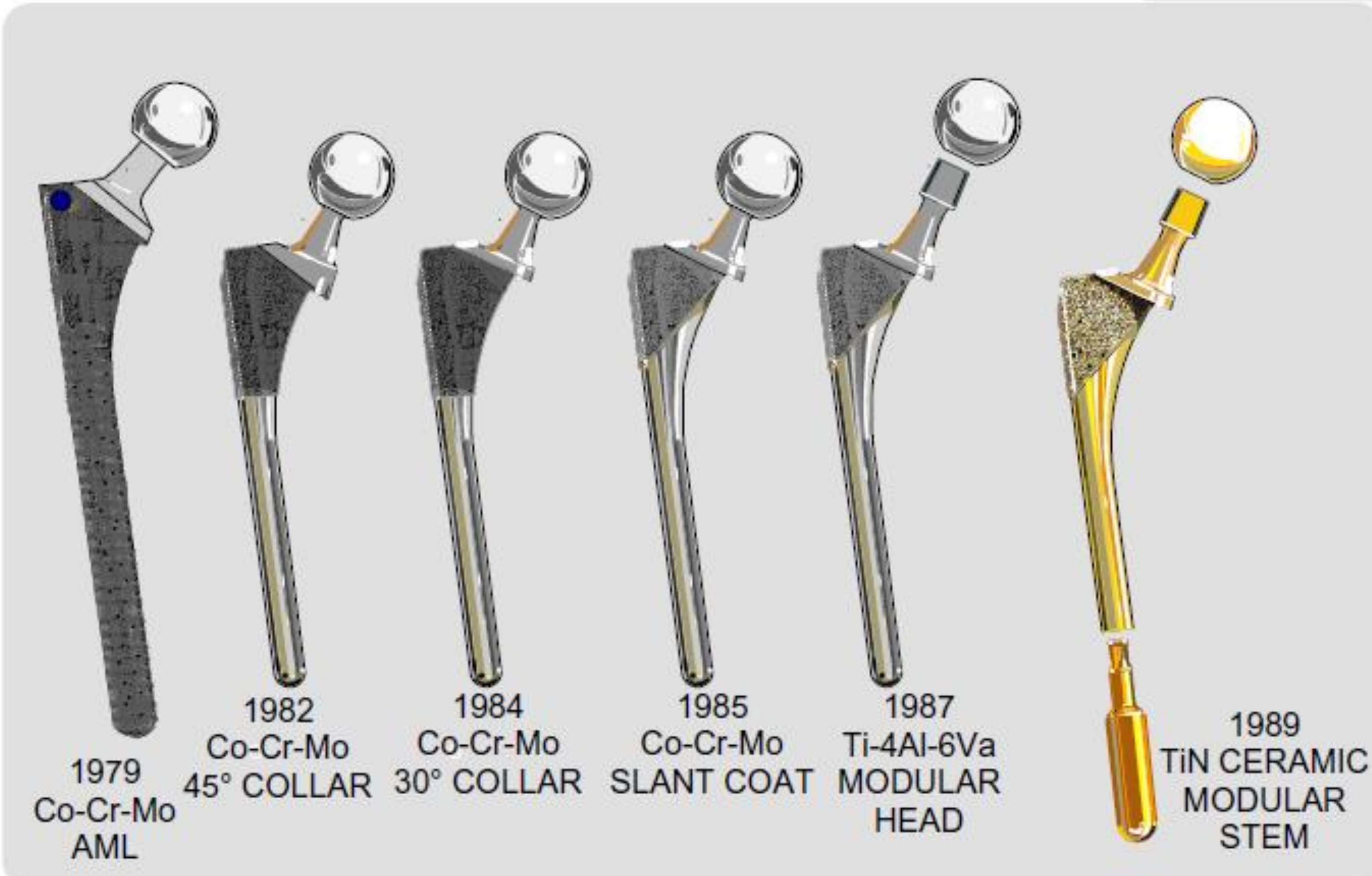

Evolution of Proximally Porous Coated Femoral Components for Hip Joint Replacement.

The Femoral Stem Components

a) Neck Alignment: align of the neck to the peak load vector

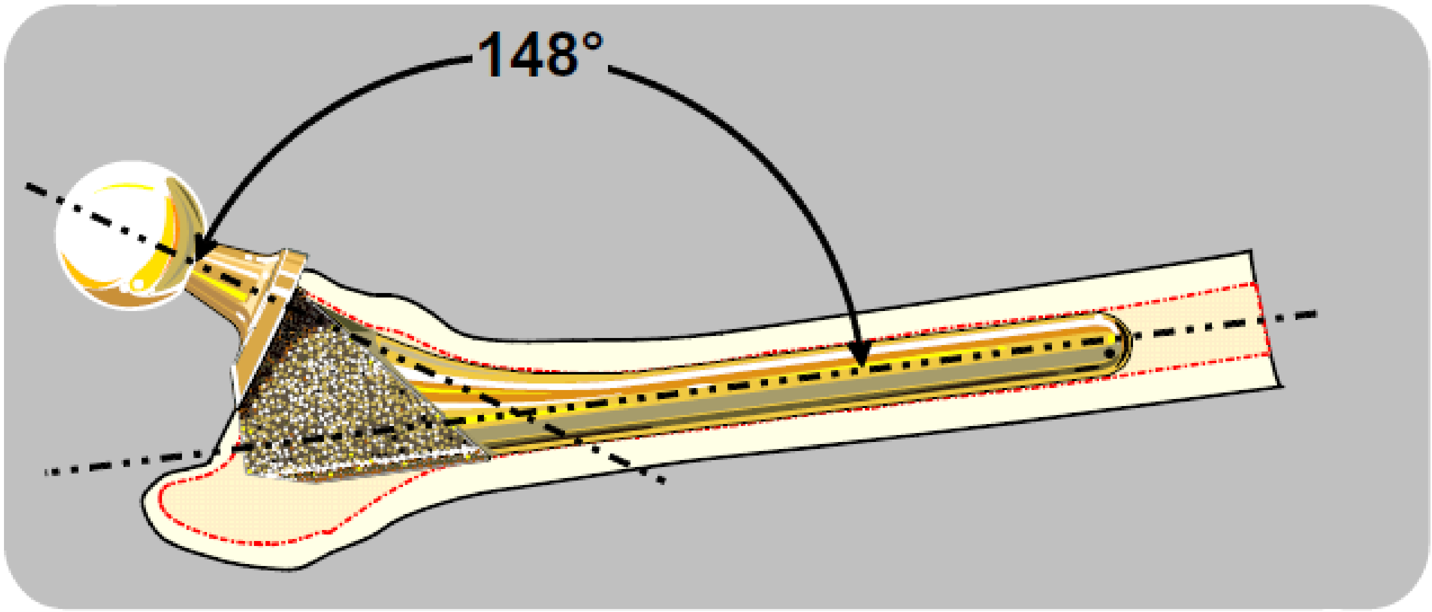

The Buechel-Pappas Femoral Stem to Neck Angle. During the peak load phase of normal walking the vector is at an angle of about 148° to the axis of the stem. A femoral shaft to neck angle of about 135° is optimal for the human femur, but not for prostheses

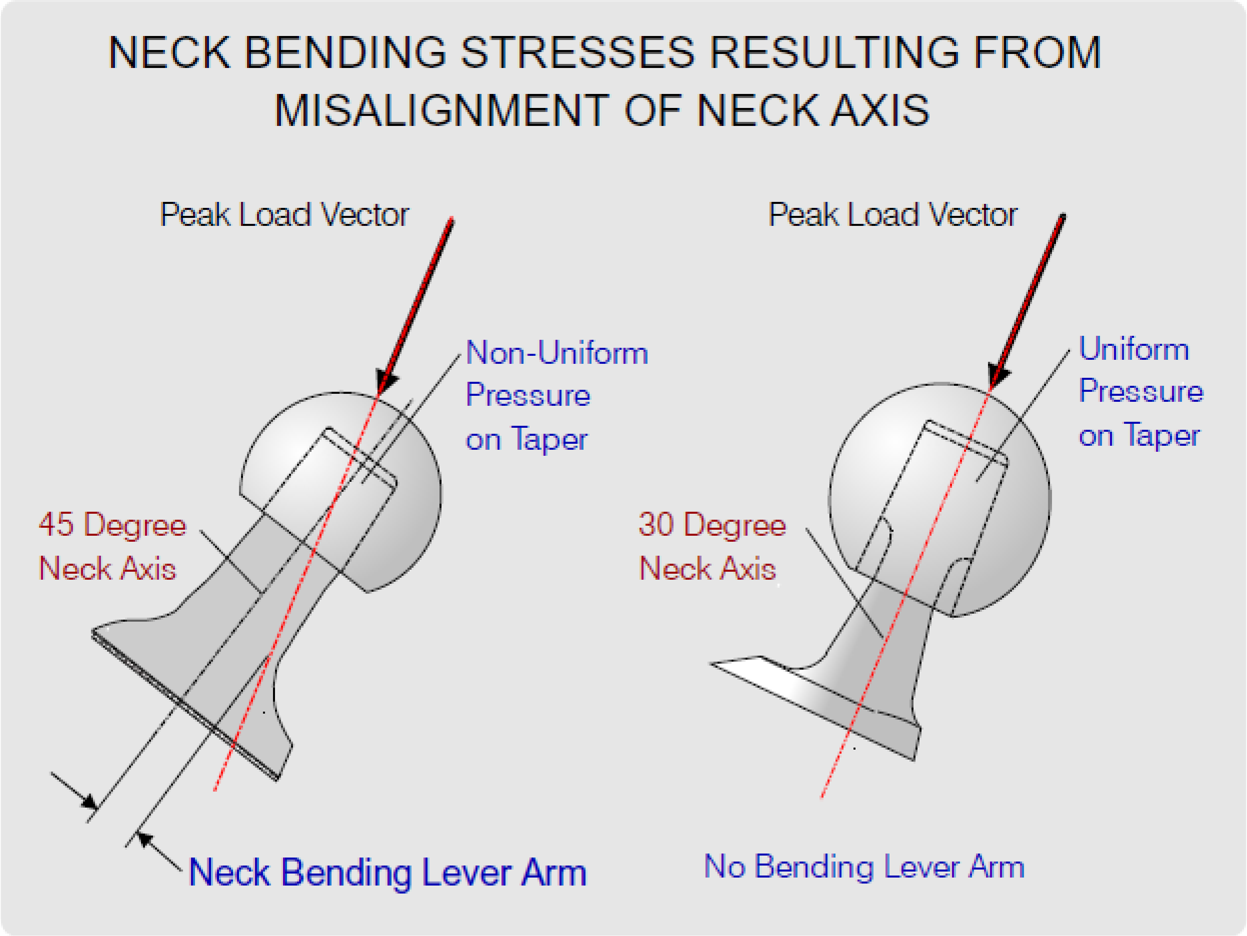

Reduction of Neck Stress

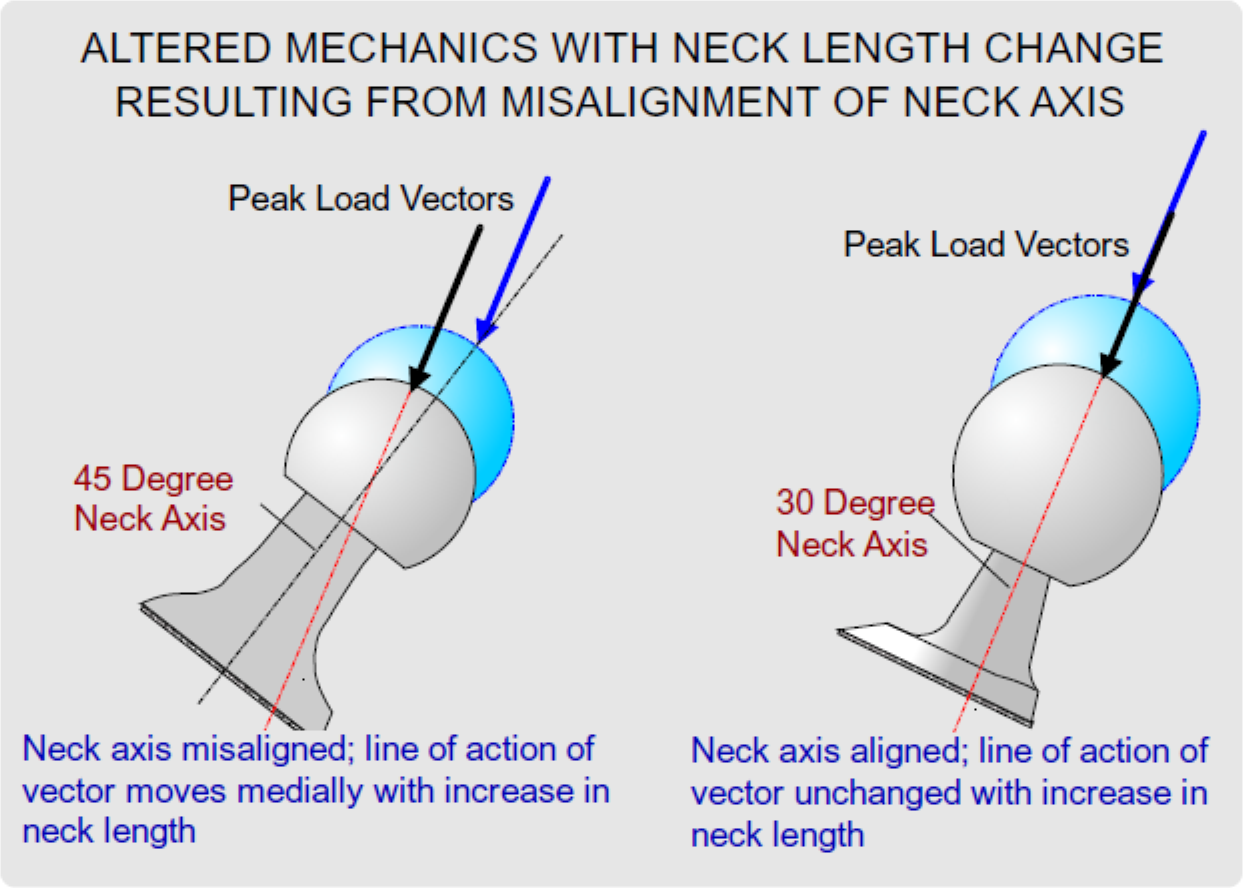

Change in the Line of Action of the Peak Load Force.

b) Head Truncation

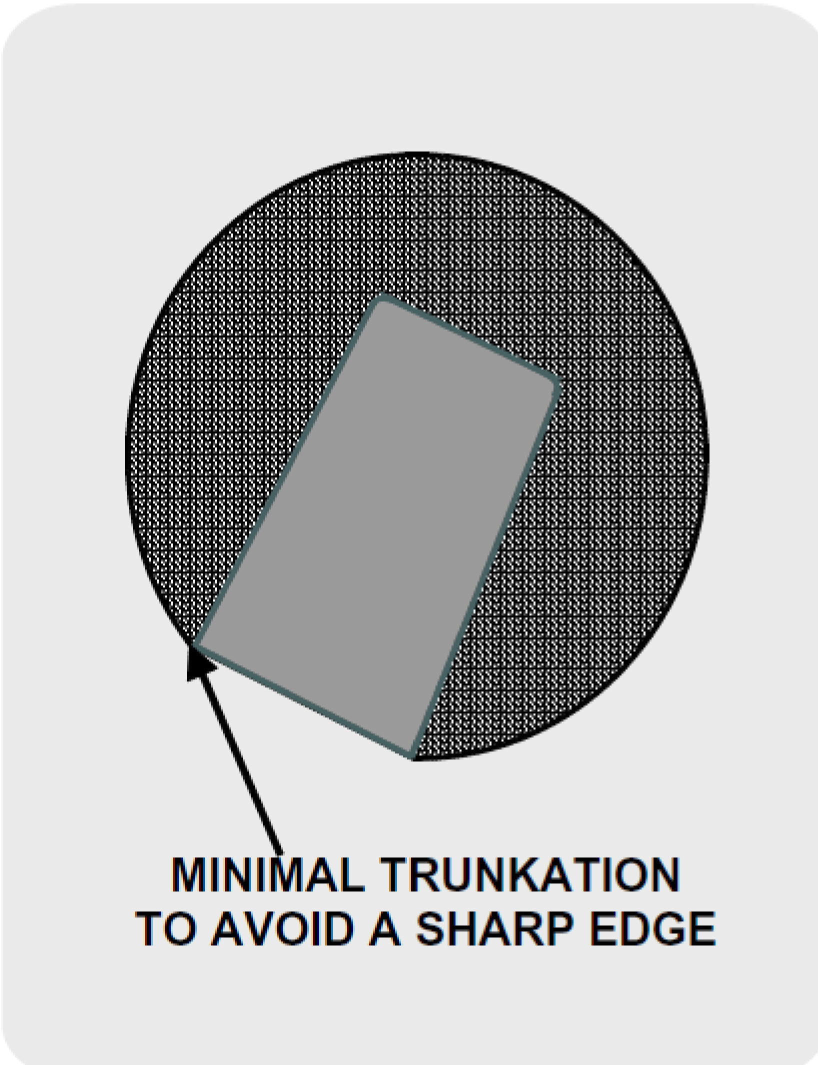

Truncation of the B-P Femoral Head

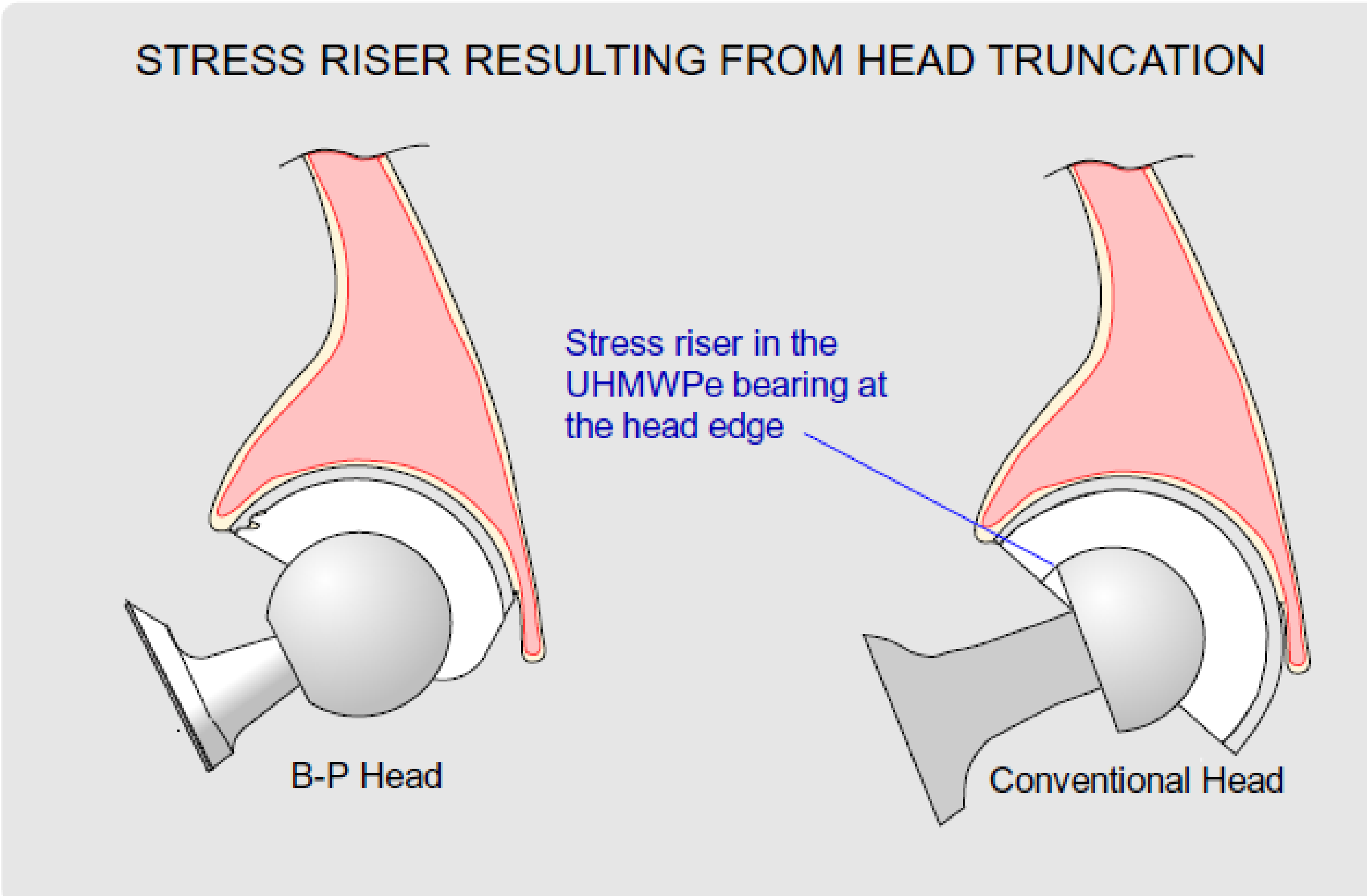

Elimination of Stress Concentration

c) Collar Angle

Reduction of Shearing Forces

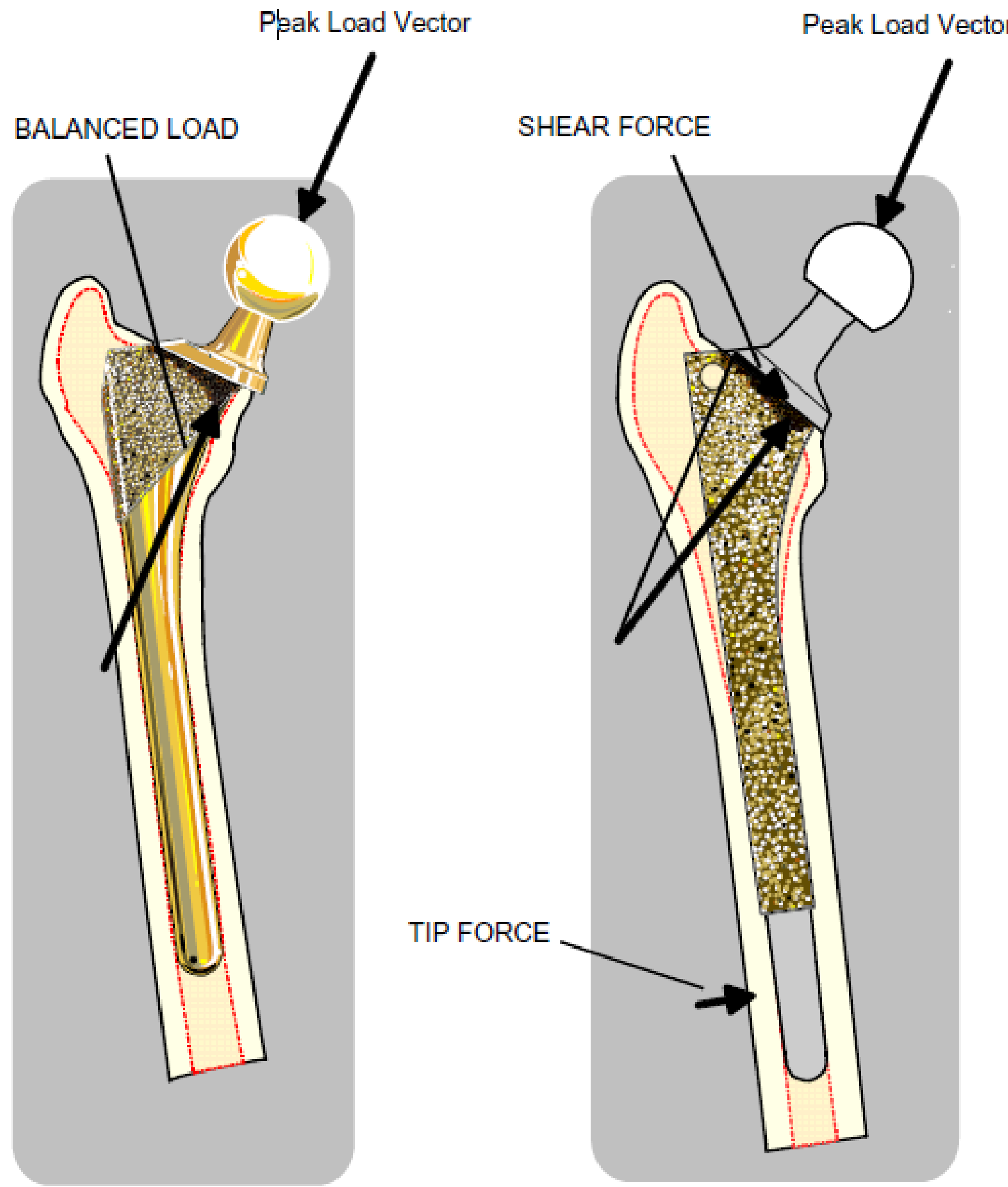

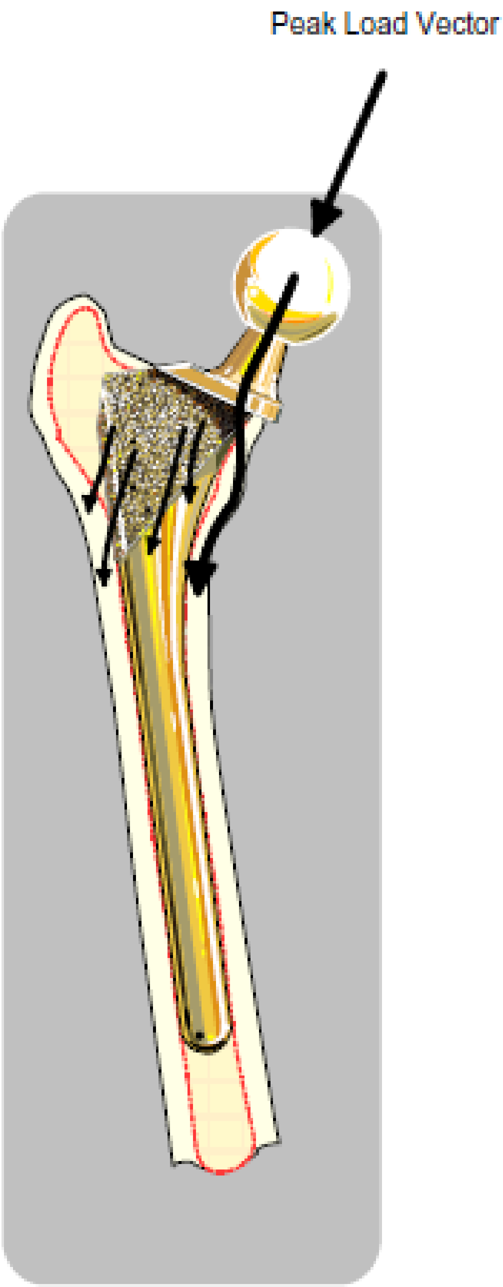

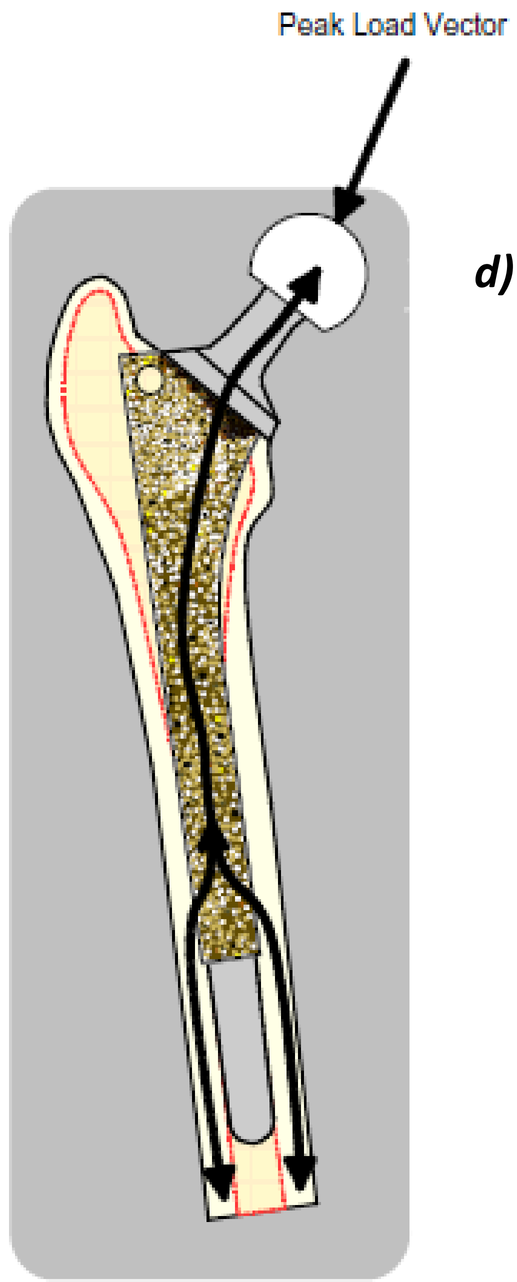

d) Inclined Proximal Porous Coating

Reduction in Proximal Stress Protection by Inclined Porous Coating

e) Proportional Sizing

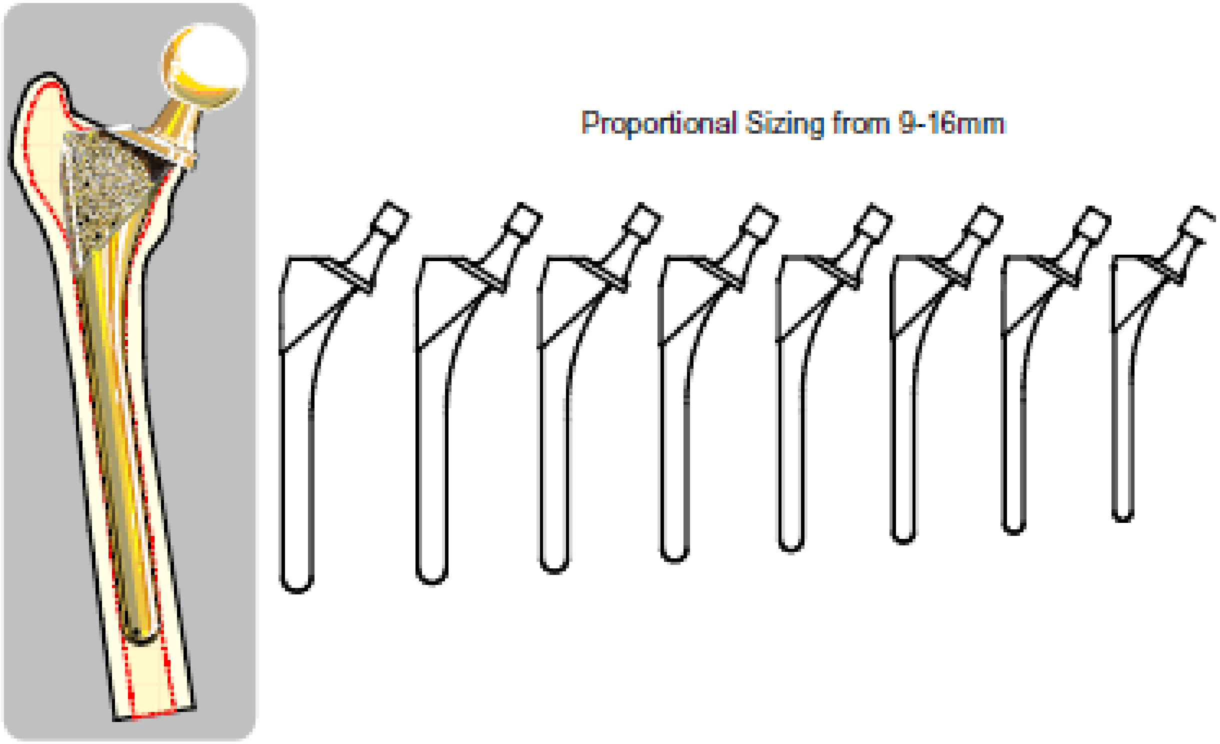

Proportional Femoral Stem Sizing

f) Ease of Removal

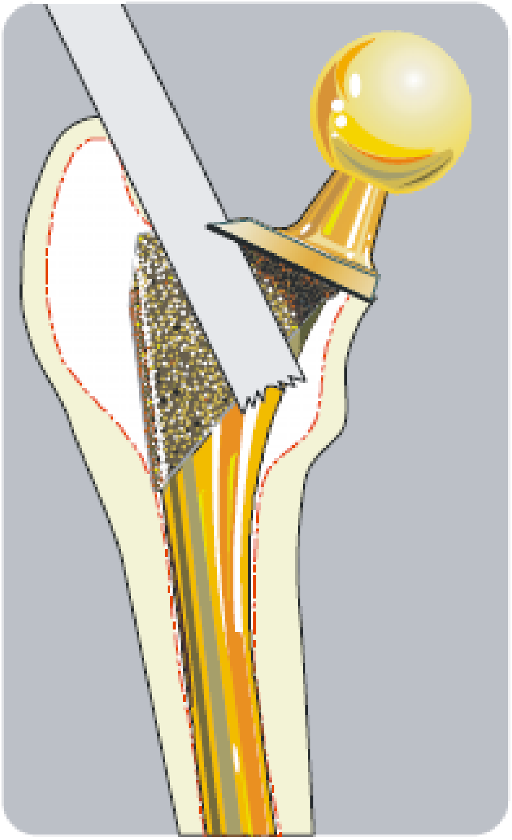

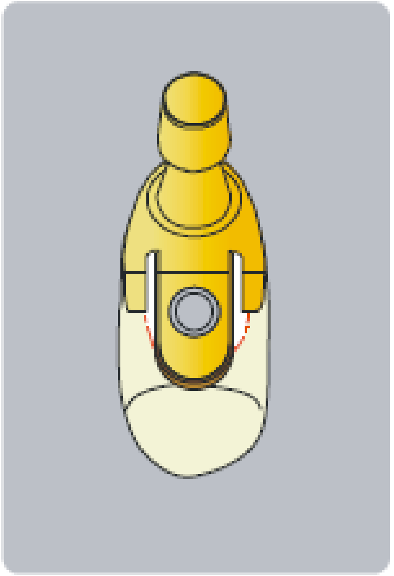

g) Titanium Alloy and Ceramic TiN Coating

TiN (Titanium nitride) Ceramic Coated
Titanium Alloy B-P Femoral Stem

Ti:
Mechanically compatible
Biocompatible more than Co-Cr alloys
Better fatigue and yielding resistance
But: inferior abrasion resistance

TiN ceramic coatings: extreme
hardness, and abrasion resistance

TiN Ceramic Coated Titanium Femoral Taper and Head

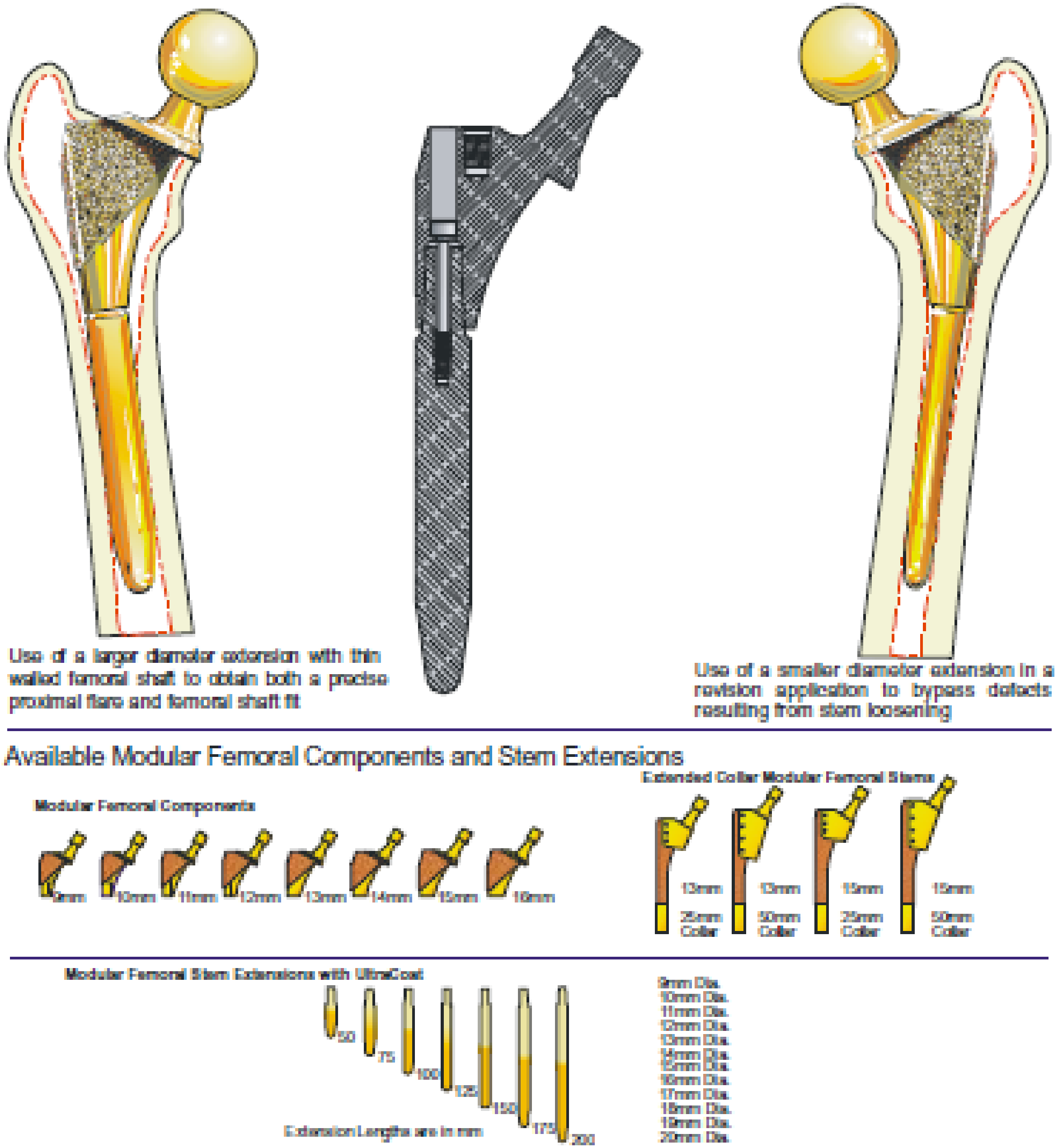

h) Modular Femoral Stem and Stem Extensions

i) Strength Analysis and Testing

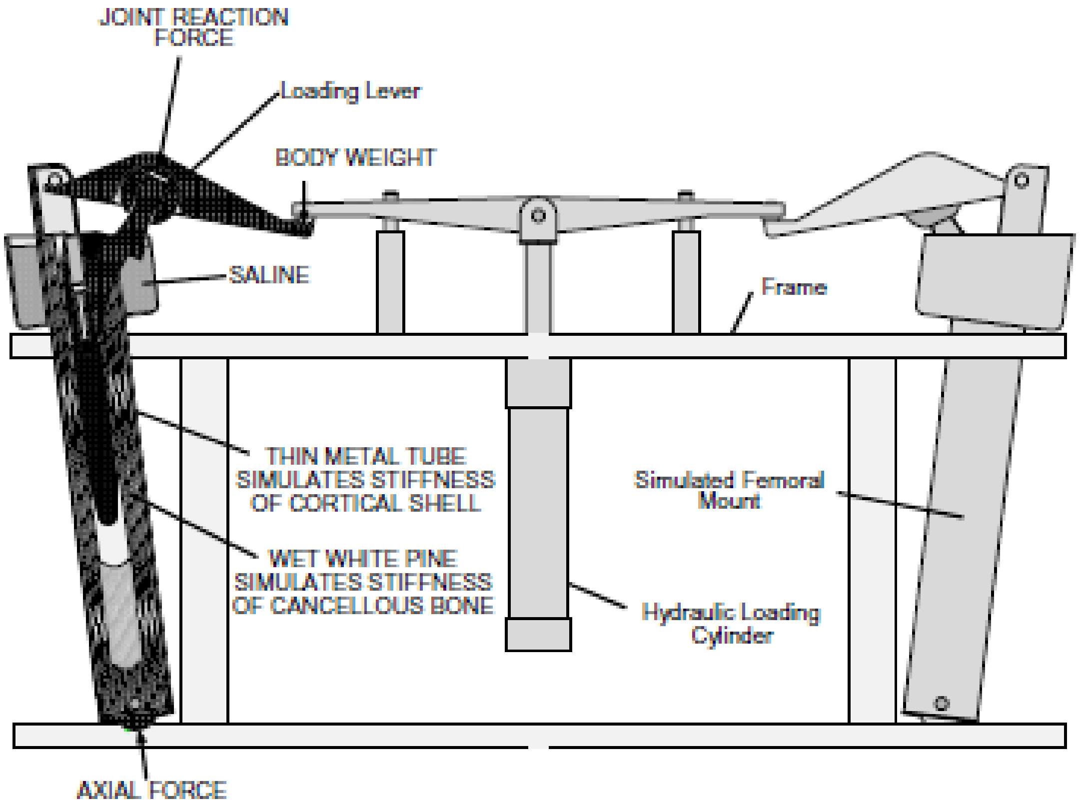

Hip Loading Simulator

The Acetabular Components

The fixed acetabular component uses a sintered bead, porous coated Ti-alloy outer shell of a partial hemi-spherical configuration and a “snap in” UHMWPe bearing.

B-P Acetabular Components.

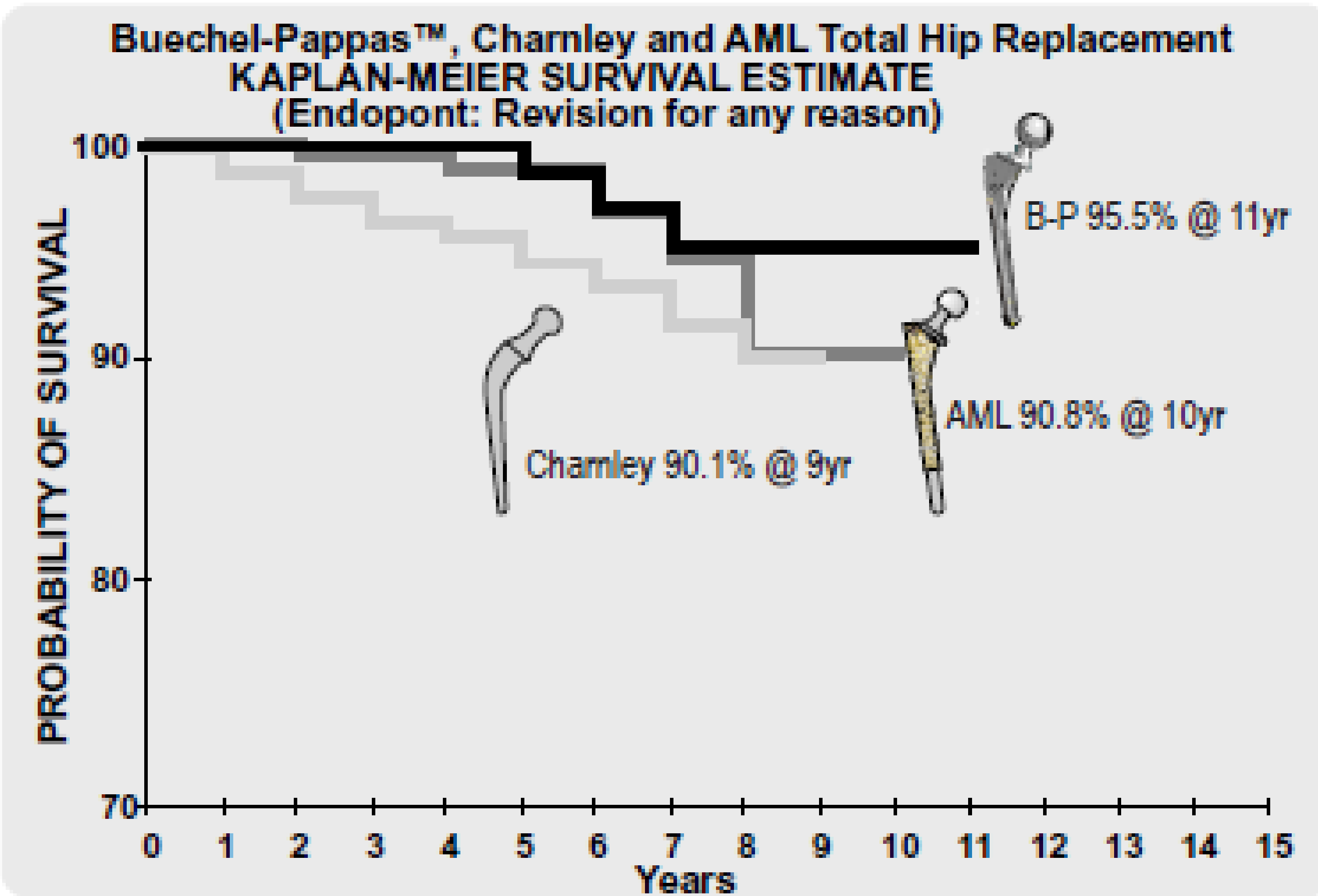

Comparison of survival of Typical Third, Fourth and Fifth Generation Total Hip Arthroplasties.

Bone conserving hip replacement

- A smaller diameter head is used and supported by a plate that is held by a bolt and short plate.
- This implant uses no cement. Benefit from having the implant coated with hydroxyapatite, the natural mineral of bone.
- The major advantage of both these designs is that they allow a traditional hip to be inserted at a subsequent operation without any great difficulty. Bone-conserving hips are more expensive than the traditional replacement.

MacMinn design (Birmingham)

Thrust plate design (Switzerland)

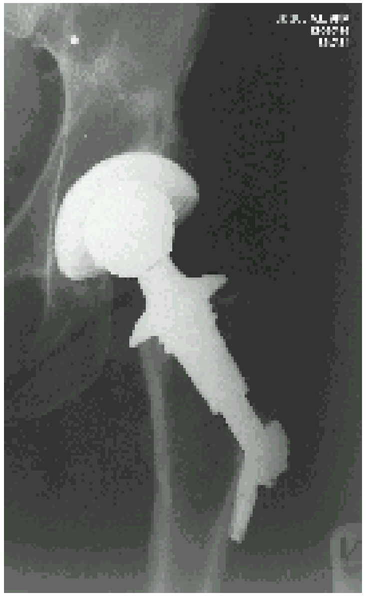

3-D stress analysis in the hip joint

Photoelasticity (double refraction): Stress distribution imaging

FEM model of femur: stresses

Reconstruction and analysis of the femur geometry in 3D

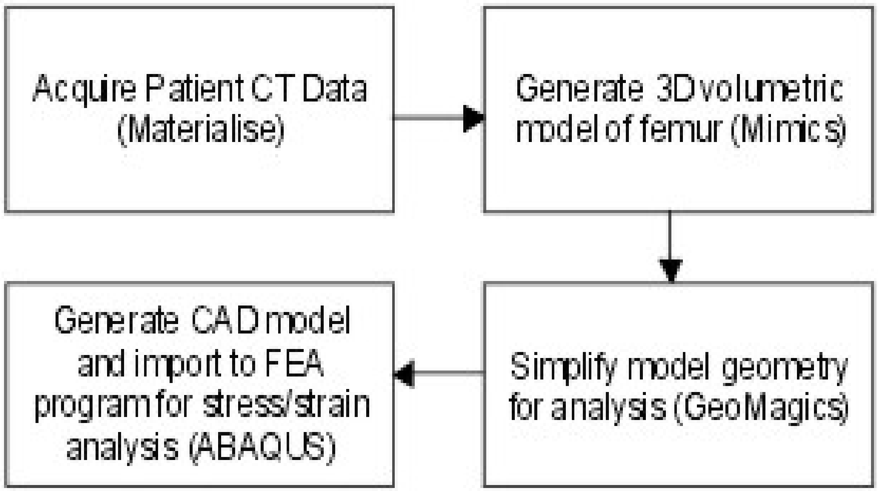

Z406 Rapid Prototyping System

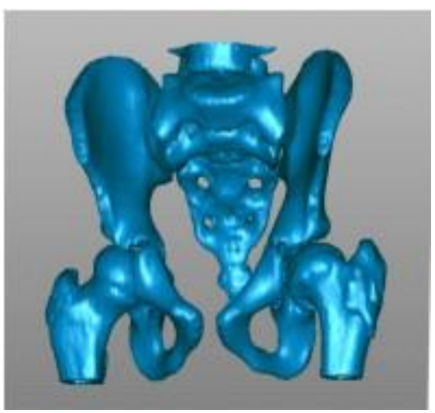

Hip assembly 3-D image generated in MIMICS

Hip assembly prototype

COUPLING STRESS ANALYSIS OF JOINTS WITH HUMAN GAIT TO IMPROVE WEAR PREDICTION IN JOINT REPLACEMENTS

Chad B. Hovey, Jean H. Heegaard, Gary S. Beaupré, Felix E. Zajac

Rehabilitation Research & Development Center
VA Palo Alto Health Care System
3801 Miranda Avenue, Palo Alto, CA 94304

Biomechanical Engineering Division
Mechanical Engineering Department
Stanford University, Stanford, CA 94305

Wear of the polyethylene bearing surface is a significant factor limiting the longevity of total joint arthroplasty. Wear is a product of contact pressure and interface sliding, which are ultimately a result of human movement. To accurately quantify the stress and deformation of the arthroplasty, the stress analysis of the joint should reflect the dynamic environment of human motion.

Many analyses utilize either rigid body gait models or deformable body joint models, but not both. Rigid body gait models can predict joint motion and forces, and help identify healthy and pathological movement [1]. However, the rigid body assumption does not allow joint stress and deformation to be determined.

Finite element models can produce joint stress and deformation, useful for predicting wear of arthroplasty [2]. However, the boundary conditions are defined *a priori* and thus may not accurately reflect the loading encountered during human movement.

In contrast to these two approaches, a coupled approach can calculate rigid body motion and joint stress in a single analysis.

Objective

- To develop a computational biomechanical model coupling a deformable diarthrodial joint to a dynamic model of human gait

Methods

Model

- Rigid body ballistic gait model
  m_{leg} = 11.72 kg, m_{HAT} = 54.23 kg, I_{leg} = 0.7479 kg-m^2
- Deformable mesh of femoral head, 160 plane strain elements
  cortical bone, E=15 GPa, ν = 0.30
  robust material law
- Constraint elements coupling rigid and deformable bodies
- Initial conditions
  stance leg
  $q_3 = 20°$
  $\dot{q}_3 = -93°/s$
  swing leg
  $q_6 = -20°$
  $\dot{q}_6 = 8°/s$

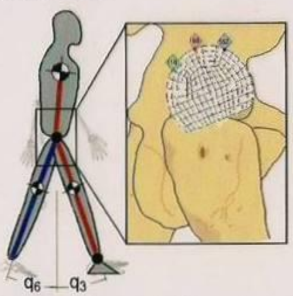

Figure 1 Coupled ballistic gait model

Measurements

- Compute dynamics of the coupled system
- Calculate stress and deformation in the hip joint

Analysis

- Compare coupled system to purely rigid classical ballistic gait
- Identify how stress in joints evolves during the gait cycle

Results

- In Fig. 2 (a-c), the large-scale motion of the coupled system (discrete points) remains nearly identical to the purely rigid system (continuous color curves).
- The angular positions of the stance and swing legs alternate between -20° and 20°, creating one ballistic gait cycle (Fig. 2a). Multiple gait cycles would have continuous angular positions but discontinuous angular velocities (Fig. 2b).
- Fig. 2c shows the hip joint reaction force in the vertical direction to peak at 600 N. The horizontal hip reaction force initially is at -200 N, goes through zero at mid-stance, and ends at 200 N.
- Figs. 2d-3 show the hydrostatic pressure is highest on the cranial portion of the femoral head (node 198). Regions of low hydrostatic pressure move from anterior (node 182) to posterior (node 118) as the stance leg moves from beginning of stance (Fig. 3, 0.0 s) to end of stance (Fig. 3, 0.6 s).

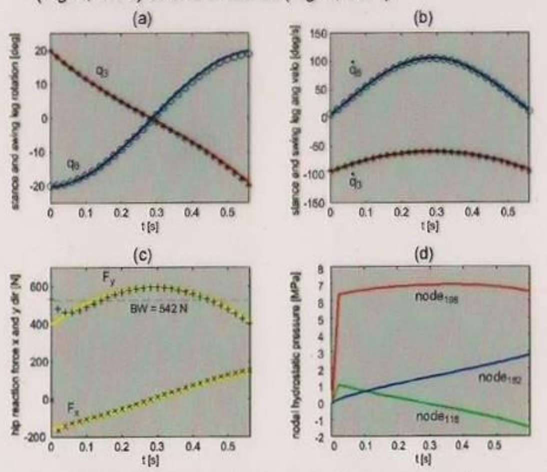

Figure 2 Coupled vs. purely rigid system results

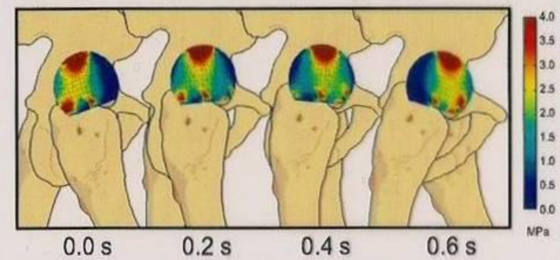

Figure 3 Hydrostatic pressure evolution during stance

Discussion

The similarity in the dynamics of the coupled system to the purely rigid system indicates that deformation of the joint has a negligible effect on the dynamics of the gait simulation. This result supports the assumption that the deformable joint plays an insignificant role in the dynamics of gait. In addition to testing the assumptions of purely rigid models, the coupled framework could also validate purely deformable joint models to assure the applied loads are consistent with the dynamics of human motion.

The joint stress is lower than physiological values because ballistic gait models do not use muscles. Including the co-contraction of muscles would result in higher joint stresses. This result indicates that the role of muscle co-contraction may be as significant as the role of gait dynamics in the calculation of joint stress.

The computational framework can use patient-specific anthropometric and gait data from a motion analysis laboratory as inputs. The model could then predict *in vivo* joint stress for a particular patient. The results could be used to test the hypothesis that a person will adopt a locomotion strategy to minimize joint stress.

Summary

- Coupling rigid and deformable body analysis can lead to a better understanding of how the dynamics of gait cause stress and deformation in joints.
- Improved knowledge of stress and deformation in joints can be helpful for improving total joint arthroplasty design.

References: [1] Andriacchi *et al.*, Basic Orthop. Biomech., 37-67, 1997. [2] Kurtz *et al.*, J. Biomech., 967-976, 1999.

Acknowledgements: Supported by VA Pre-Doctoral Fellowship

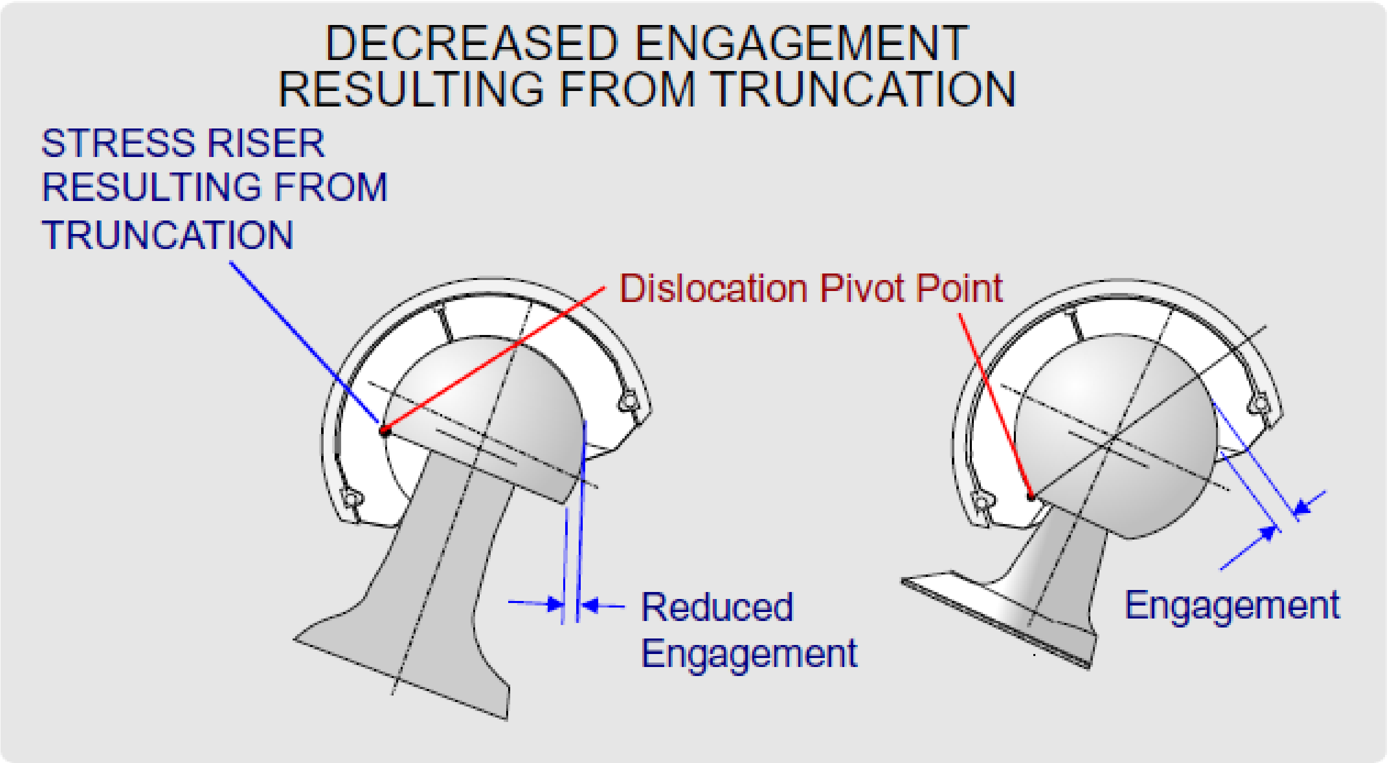

Improvement in Separation Resistance